The impact of ship emissions on air quality and human health in the Gothenburg area - Part I: 2012 emissions

Lin Tang[1,2], Martin O.P. Ramacher[3], Jana Moldanová[1], Volker Matthias[3], Matthias Karl[3], Lasse Johansson[4], Jukka-Pekka Jalkanen[4], Katarina Yaramenka[1], Armin Aulinger[3], Malin Gustafsson[1]

[1]IVL, Swedish Environmental Research Institute, P.O. Box 530 21, 40014 Gothenburg, Sweden
[2]WSP Environment Sweden, Box 13033, 402 51 Gothenburg, Sweden
[3]Chemistry Transport Modelling, Helmholtz-Zentrum Geesthacht, 21502, Geesthacht, Germany
[4]Finnish Meteorological Institute, P.O. Box 503, 00101 Helsinki, Finland

Correspondence to: Jana Moldanová (jana.modanova@ivl.se) and Lin Tang (lin.tang@wsp.com)

Abstract. Ship emissions in and around ports are of interest for urban air quality management in many harbour cities. We investigated the impact of regional and local ship emissions on urban air quality for 2012-year conditions in the city of Gothenburg, Sweden, the largest cargo port in Scandinavia. In order to assess the effects of ship emissions, a coupled regional and local-scale model system has been set up, using ship emissions in the Baltic Sea and the North Sea, as well as in and around the port of Gothenburg. Ship emissions were calculated with the Ship Traffic Emission Assessment Model (STEAM) model, taking into account individual vessel characteristics and vessel activity data. The calculated contributions from local and regional shipping to local air pollution in Gothenburg were found substantial, especially in areas around the city ports. The relative contribution from local shipping to annual mean NO_2 concentrations was 14 % as the model-domain average, meanwhile the relative contribution from regional shipping at the North Sea and the Baltic Sea was 26 %. In an area close to the city terminals, the contribution of NO_2 from local shipping (33 %) was higher than that of the road traffic (28 %), which indicates importance of controlling the local shipping emissions. The local shipping emissions of NO_x led to decreasing of the summer mean O_3 levels in the city by 0.5 ppb (~2%) in average. The regional shipping lead to a slight increase in the O_3 concentrations, however, the overall effect of the regional and the local shipping together was a small decrease of the summer mean O_3 concentrations in the city. In addition, VOC emissions from local shipping compensate up to 4 ppb decreasing of summer O_3 concentrations due to the NO titration effect. For $PM_{2.5}$, the local ship emissions contributed only 3 % to the annual mean in model domain, while regional shipping under 2012 condition was a larger contributor with an annual mean contribution of 11 % on the city-domain average.

Based on the modelled local and regional shipping contributions, the health effects of $PM_{2.5}$, NO_2 and ozone were assessed using the ALPHA-RiskPoll (ARP) model. An effect of the shipping-associated $PM_{2.5}$ exposure in the modelled area was a mean loss of the life expectancy by 0.015 years per person. The relative contribution of the local shipping to the impact of total $PM_{2.5}$ was 2.2 % which can be compared to 5.3 % contribution from the local road traffic. The relative contribution of the regional shipping was 10.3 %. The mortalities due to the exposure to NO_2 associated to shipping were calculated to be 2.6 premature deaths/year. The relative contribution of the local and the regional shipping to the total exposure to NO_2 in the reference simulation was 14 % and 21 %, respectively. The shipping related ozone exposures were due to the NO titration effect, leading to negative number of premature deaths. Our study shows that overall health impacts of regional shipping can be more important than those of local shipping, emphasizing that abatement policy options on city-scale air pollution require close cooperation across governance levels. Our findings indicate that the strengthened Sulphur Emission Control Areas (SECA) fuel sulphur limit from 1 % to 0.1 % in 2015, leading to strong decrease in formation of secondary particulate matter on regional scale, has been an important step in improving of the air quality in the city.

65

70

75

80

85

90

1 Introduction

Shipping is an important source of air pollutants, both on the global and European level (Corbett et al., 1999; Eyring et al., 2005; Cofala et al., 2007). The most important species emitted are sulphur oxides (SO_x), nitrogen oxides (NO_x), particulate matter (PM) and to some extent carbon monoxide (CO) and volatile organic compounds (VOC). Since nearly 70 % of ship emissions occur within 400 km of coastlines (Corbett et al., 1999), the largest contributions of shipping to air pollution are concentrated to coastal regions with intensive ship traffic and to harbours, where emissions from harbour operations add further to the air pollution generated by ships. The primary air pollutants from shipping contribute to the formation of secondary air pollutants, mainly ozone and secondary particulate matter. On average shipping emissions contributed with 9.4 % to concentrations of primary $PM_{2.5}$ (particulate matter with a median aerodynamic diameter less than or equal to 2.5 µm) and with 12.3 % to concentration of secondary inorganic particulate matter over the Europe during 1997–2003 (Andersson et al., 2009).

Emissions from the international shipping are controlled through International Maritime Organisation (IMO) and regulations included in the International Convention on the Prevention of Pollution from Ships (MARPOL 73/78) and its annexes. The MARPOL Annex VI- "Regulations for the Prevention of Air Pollution from Ships" sets limits for emissions of SO_x and NO_x. Sulphur is regulated through maximum allowed sulphur content in the fuel used, while NO_x is regulated through Tier limits for maximum specific emissions of NO_x from each engine on board. The limits depend on the nominal rotation speed of an engine and different Tiers apply for ships built or substantially re-built in different time periods (2000–2011 Tier 1, after 2011 Tier 2). For fuel sulphur content (FSC) a global limit of 0.5 % applies since 1st January 2020, before it was 3.5 %. However, the Baltic Sea, the North Sea and the English Channel are so called Sulphur Emission Control Areas (SECA) where stringer limits apply: in July 2010 it was decreased from 1.5 % to 1.0 %, which is also the limit that applies in this study. In 2015 the fuel sulphur limit was decreased further to 0.10 %. In addition, since 2010 a sulphur content limit of 0.10 % for fuels used by ships at berth for a period longer than 2 hours applied for all EU ports. Sweden has also introduced economic incentives for reduction of the shipping emissions in form of differentiated fairway and port fees with a discount for ships using emission control technologies, contributing to a relatively large share of ships with NO_X abatement technology in the region. In 2020 the global cap for the FSC will be decreased to 0.50 %. In 2021 a Nitrogen Emission Control Area (NECA) will enter in force in this area with mandatory Tier 3 standard (80 % reduction comparing to Tier 1) for ships built in 2021 and later operating in the region.

In the Baltic Sea and the North Sea an intensive ship traffic results in high emissions of air pollutants and contributes to high atmospheric concentrations of particularly of NO_x in and around several major ports (Jonson et al., 2015). The relative contribution of shipping in the North Sea and Baltic Sea to coastal NO_2 concentrations are highest along the coasts of southern Sweden, the south-western coast of Finland, and the coast of Estonia, 25–40 % on annual average (Jonson et al, 2019). Jonson et al. (2019) found that the Baltic Sea and North Sea shipping contributed significantly also to concentrations of particulate

matter (highest contributions 6–12 %, allocated to similar areas as NO_x) and to the deposition of sulphur (highest contributions 10–20 %), before the strengthening of SECA fuel sulphur limit. They have also shown that the strengthened limit on the fuel S content in 2015 from 1.0 % to 0.10 % brought a significant decrease in emissions as well as contributions of shipping to air pollution by SO_2 and to S deposition (maximum contribution about 2 %) and to a reduction of shipping contribution to the concentrations of PM. Aulinger et al. (2016) and Matthias et al. (2016) studied impacts of the current and future (2030) North Sea shipping on air pollution and found contributions consistent with Jonson et al. (2019) (highest NO_2 contributions 25 % and 15 % in summer and winter, respectively, ozone increased by 10% along Scandinavian coast). By 2030, the contribution of shipping to the NO_2 and O_3 concentrations was estimated to increase by more than 20 % and 5 %, respectively, due to the expected enhanced traffic, if no regulation for further emission reductions is implemented in the North Sea area (Matthias et al., 2016).

Several studies have assessed impacts of shipping on human exposure to air pollutants and associated to health impacts. Andersson et al. (2009) assessed impacts of different source regions and also of emissions from international shipping on personal exposure and to the relative increase of death rates from exposure to particulate matter across Europe with help of the atmospheric chemistry-transport model MATCH. They found that shipping, before the introduction of a SECA in the region, contributed with 5 % to population-weighted average concentration (PWC) of primary $PM_{2.5}$ and with 9 % to PWC of secondary inorganic particles. For individual countries in Northern Europe the contribution to PM exposure varied between 3 % and 19 %. Jonson et al. (2015) assessed health impacts of $PM_{2.5}$ associated to emissions from ships in the Baltic Sea and the North Sea in years 2009 and 2011, i.e. before and after the SECA FSC limit was strengthened from 1.5 % to 1.0 %, with help of EMEP chemistry-transport model. The relative contributions of shipping to population exposure to $PM_{2.5}$ were found between 1.6 % and 12 % for 2009, and 1.4 % and 10 % for 2011 for the riparian countries, decreasing by 0–40 % between these years in the different countries. Contributions from shipping to the total exposure to particles in these countries found by Jonson et al. (2015) for year 2009 were by 14–64 % lower than those found in Andersson et al. (2015), accounting that, apart from differences in models and meteorological years used in the 2 studies, Andersson et al. assessed impact of all European shipping prior to SECA regulation entered into force while Jonson et al. assessed impact of the Baltic Sea and the North Sea shipping after the introduction of the 1.5 % SECA fuel sulphur content limit. Barregård et al. (2019) assessed impact of shipping in the Baltic Sea for emission years 2014 and 2016, i.e. before and after strengthening of SECA FSC limit from 1.0 % to 0.1 % using the EMEP model and showed that exposure to $PM_{2.5}$ associated to the Baltic Sea shipping decreased by 34 % in the region due to this abatement measure, using emissions representative for year 2016, shipping contributed with 10 % to the population exposure of $PM_{2.5}$ in the coastal regions but only less than 1 % in more remote inland areas.

The methodologies for calculation of the health impacts of $PM_{2.5}$ in the above discussed studies vary both in the exposure response functions (ERF) used and how the years of life lost are calculated from statistics of mortalities and life-tables. The

most common ERF used is the one recommended by the HARPIE study (WHO, 2013a), increased risk of all-cause mortality 1.0062 (95 % CI 1.004–1.008) per µg/m^3, which is almost the same as ERF from Poppe et al. (2002). Several studies use a higher ERF presented in Jerret et al. (2005) and in the ESCAPE study (Beelen et al., 2014), both of very similar value, the latter being 1.014 (95 % CI 1.004–1.026) per µg/m^3. Andersson et al. (2009) calculated increase of death rates from exposure to particulate matter in Europe using ERF from Poppe et al. (2002) for the secondary inorganic aerosol and ERF from Jerret et al. (2005) for the primary PM$_{2.5}$, reasoning that the ERF of Jerret et al., based on intra-city gradients is better representing the impact of primary PM$_{2.5}$, while Poppe et al. uses the inter-city differences reflecting more impact of secondary PM. Combining the increase of mortality from particulate matter in EU27 and the relative contribution of shipping to the exposure to primary and secondary inorganic PM, Andersson et al. (2015) found the resulting impact of shipping on mortality 22 000 premature deaths per year. Jonsson et al. (2015) used the RAINS methodology which calculates years of life lost (YOLLs) over the expected lifetime of population in risk, in this case population above 30 years, accumulating YOLLs between the ages of 30 and c.a. 80 years (Amann et al., 2004). The RAINS methodology uses ERF recommended by the HARPIE project. As a result, Jonson et al. (2015) estimated 0.1–0.2 YOLLs per person in areas close to the major ship tracks resulting from the ship emissions in the Baltic Sea and the North Sea for year 2010. Barregård et al. (2019) estimated that 187-421 premature deaths per year, corresponding to 0.01–0.02 YOLLs per person, could be associated with contributions of the Baltic Sea shipping emissions to concentrations of PM$_{2.5}$ in year 2014. The lower and higher estimates used ERF from WHO (2013) and Beelen et al. (2014), respectively. In our study the impacts of exposure to shipping-related air pollutants on health of people living in the Gothenburg region have been assessed using the ALPHA-RiskPoll methodology (ARP, Holland et al. 2013, Åström et al., 2018) which uses the ERFs from the HARPIE project (WHO, 2013a).

The city of Gothenburg is located on the western coast of Sweden, with about 0.57 million inhabitants and an area of 450 km^2. The dominant wind direction in Gothenburg is south-west with average wind speed of 3.5 m s^{-1}, indicating the major transport path from sea to the land, especially in summer. The geomorphology of the Gothenburg area is described as a fissure valley landscape dominated by a few large valleys in north-south and east-west directions. The major air pollution sources in Gothenburg are above all road traffic and industry, wood burning, shipping, agriculture, working machines and long-range transport (LRT) from the European continent and other parts of Sweden. The harbour and shipping activities are important emission sources and directly influences the urban air quality. The centre of the city is situated on the southern shore of the river Göta älv. The Port of Gothenburg receives between 6,000 and 6,500 calls per year and additional 600–700 ships pass to and from ports upstream and on the Göta älv. The port annually handles approximately 900,000 containers, 20 million tonnes of petroleum, and half a million Roll-on/roll-off (RoRo) units (Winnes et al., 2015). Passenger traffic in Gothenburg is also very busy with 1.5 million passengers who ferry to and from Gothenburg to Denmark, Germany *etc.* on Stena Line ferries each year. This makes the port the largest cargo port in Scandinavia.

Comparing with other European cities, the air pollution levels in Gothenburg are low and the air quality has become better and better since the 70s because of the effective emission control addressing industry and road traffic. The trends of SO_2, NO_x and NO_2 have been continuously decreasing from 1990 to 2015, except for the areas close to major roads (Miljöförvaltningen, 2017). O_3 exhibits an increasing trend and there is also a slowly increasing trend for PM_{10} in Gothenburg (Olstrup et al., 2018). The annual means for NO_2, PM_{10} and $PM_{2.5}$ (particulate matter with aerodynamic diameter less than or equal to 10 µm and 2.5 µm, respectively) during the period 2000–2017 are 12.5 ppb, 16.3 µg/m^3 and 7.9 µg/m^3, respectively, at an urban background site in Gothenburg. The decreased levels of NO_x and NO_2 during the period 1990–2015 in Gothenburg were estimated to increase the life expectancy by up to 12 months and 6 months respectively, and the slight increased trend of O_3 and PM_{10} have relatively little impact on life expectancy (-2 month and -1 month) (Olstrup et al., 2018). In terms of exposure to PM_{10} and $PM_{2.5}$ from different source categories in Gothenburg, Segersson et al. (2017) calculated that the largest part was due to the long-range transport and the dominating local sources were road traffic and residential wood combustion, while the contribution from local shipping was small, 0.04 µg/m^3 population weighted annual mean $PM_{2.5}$. The exposure of $PM_{2.5}$ from shipping in other harbour cities in Sweden are lower than in Gothenburg, with 0.02 µg/m^3 in Stockholm and 0.01 µg/ m^3 in Umea (Segersson et al., 2017).

This study has been conducted within the BONUS SHEBA project (Shipping and Environment of the Baltic Sea Region) where the impact of current and scenario emissions from ships on air quality have been investigated as a part of a holistic assessment framework for impacts of shipping on marine and coastal environment. The shipping-related air pollution has been investigated on a range of spatial scales with several chemistry-transport models: coarse spatial scale resolution was used for simulations in the European domain, finer resolution was used for the Baltic Sea (Karl et al., 2019a, c), and city-scale simulations using high spatial resolution were used for several harbour cities (Ramacher et al., 2019a). The present study (Part I) evaluates the contributions of regional and local shipping to the concentrations of SO_2, NO_2, $PM_{2.5}$, O_3 and secondary PM, as well as the human exposure and the associated health impacts in Gothenburg for year 2012. Health impact studies for the shipping emissions in cities are rare, mainly because the spatial resolution of the regional CTM (Chemical Transport Model) does not allow for the city-scale resolution. This study provides the city-scale Health Impact Assessment (HIA) and identifies and addresses potential health impacts associated to local and regional shipping. The studied year (2012) has been considered as a present-day "normal year" for Baltic Sea Region in terms of meteorological conditions in BONUS-SHEBA. In terms of ship emission regulations, the study presents a situation with 3.5 % FSC global limit, 1.0 % FSC limit in the SECA area whereas 0.1 % FSC limit applies for ships berthing in the port of Gothenburg or operating within the Göta älv estuary. Several alternative shipping scenarios in year 2040 are discussed further in Ramacher et al., 2019b (Part II).

2 Methodology

2.1 Model set-up

For the city-scale chemistry transport model (CTM), the prognostic meteorology-dispersion model TAPM (The Air Pollution Model) (Hurley et al., 2005; Hurley, 2008 a) was used. TAPM consists of a meteorological and an air pollution components. The meteorological component of TAPM is an incompressible, non-hydrostatic, primitive equation model with a terrain-following vertical sigma coordinate for 3-D simulations. The model solves the momentum equations for horizontal wind components, the incompressible continuity equation for vertical velocity, and scalar equations for potential virtual temperature and specific humidity of water vapour, cloud water/ice, rain water and snow. The turbulence terms in these equations have been determined by solving equations for turbulence kinetic energy and eddy dissipation rate, and then using these values to represent vertical fluxes by a gradient diffusion approach (Hurley, 2008b). Using predicted meteorology and turbulence from the meteorological component, TAPM applies Eulerian grid module in its air pollution component which consists of nested grid-based solutions of the Eulerian concentration mean equations representing advection, diffusion, chemical reactions and emissions. Dry and wet deposition processes for gases and PM are also included. It includes gas-phase photochemistry based on the Generic Reaction Set (Azzi et al., 1992), gas- and aqueous-phase chemical reactions for SO_2, formation of ozone from NO_X and NMVOC (treated as VOC reactivity). The photochemistry mechanism captures also the important features of the secondary particle formation, i.e. formation of sulphate and nitrate following the SO_2 and NO_2 oxidation, as well as formation of secondary organic aerosol as a fixed part of the degraded smog reactivity representing VOC species in the reaction scheme of TAPM (Hurley, 2008b).

In this study, the meteorological component of TAPM was driven by the recently published ECMWF ERA5 synoptic meteorological reanalysis ensemble means with 30 vertical layers, $0.3° \times 0.3°$ horizontal and three-hour temporal resolution. For a time period of 2012, five nested domains have been simulated with the synoptic meteorological component with the inner-most meteorological fields of a 30 km $\times$ 30 km domain with 500 m resolution (Figure 3a). In addition, the observed wind fields at four meteorological sites were assimilated to nudge wind speed and wind direction calculations in the inner-most domain. In TAPM, an Exner pressure function is integrated from mean sea level to the model top (10 Pa in this study) to determine the top boundary condition. The Exner pressure function is determined from the sum of the hydrostatic component and non-hydrostatic component (Hurley, 2008). The number of vertical grid levels was 30 in this study. Twenty of these layers are below approximately 2 km; the lowest layer extends to ca. 10 m above ground.

The spatial resolution of the city-scale CTM was 250 m $\times$ 250 m with local coordinate system SWEREF 99 1200 and the size of the CTM domain was about 25 km $\times$ 25 km, covering the city of Gothenburg and the harbour area along shores of the Göta älv running through the city (Fig. 1a).

255 The chemical boundary conditions were taken from the Community Multi-scale Air Quality Modelling System (CMAQ) (Byun and Ching, 1999; Byun and Schere, 2006). CMAQ model simulations on a 4 km × 4 km grid (Karl et al., 2019c), which were used for the chemical boundary conditions (Fig. 1b), were driven by the high-resolution meteorology meteorological fields of the COSMO-CLM (Rockel et al., 2008) version 5.0 using the ERA-Interim re-analysis as forcing data. Chemical boundary conditions for the CMAQ model simulations were provided through hemispheric CTM simulations, from a SILAM model

260 (Sofiev et al., 2006) run on a 0.5˚ × 0.5˚ grid resolution, which was provided by Finnish Meteorological Institute (FMI). Land based emissions for the regional-scale simulations were represented by hourly gridded emissions calculated with SMOKE-EU emission model (Bieser et al., 2011). The SMOKE-EU emission data is based on reported annual total emissions from the European point source emission register (EPER), the official EMEP (www.ceip.at) emission inventory and the EDGAR HTAP v2 database (EPER, 2018; CEIP, 2018; Olivier et al., 1999). For shipping emissions, the model used an inventory calculated

265 with the STEAM model consistent with the inventory used by TAPM for the city-scale, calculated with 2 km × 2 km grid resolution (STEAM3, Johansson et al., 2017), more details are given in the next section. The STEAM model version used for the CMAQ simulations was, however, not including VOC emissions. As chemical boundary conditions, vertical model layer seven with a mid-layer height of approximately 385 m above ground was selected. CMAQ simulations with and without ship emissions in the Baltic Sea and the North Sea included were used in TAPM simulation runs. Since the TAPM allows just 1-d

270 boundary concentration fields with hourly time resolution, the TAPM boundary concentrations were calculated using the horizontal wind components on each of the four lateral boundaries for weighting the upwind boundary concentrations around the TAPM model domain (Fridell et al., 2014). The city-scale model set-up are summarised in Table 1.

2.2 Emission inventory

2.1.1 Regional and local shipping emissions

275 Shipping emissions were calculated with the Ship Traffic Emission Assessment Model taking into account individual vessel characteristics and vessel activity data (STEAM; Jalkanen et al., 2012; Johansson et al., 2017) based on detailed information of technical parameters of individual vessels and position data of individual ships taken from reports from the Automatic Identification System (AIS) of the Helsinki Convention (HELCOM) member states. The STEAM model calculated fuel consumption and emissions as a function of vessel activity, the STEAM3 version of the model has been used (Johansson et

280 al., 2017), with an additional module for calculation of VOC emissions. The emission inventory includes combustion emissions from all engines and appliances on ships (boilers, auxiliary and main engines). The emission inventory for the local shipping around Gothenburg consists of hourly emissions from ships on 250 m × 250 m grid resolution. The STEAM model provided shipping emissions for year 2012 for the compounds NO_x, SO_x, CO, CO_2, VOC and $PM_{2.5}$. $PM_{2.5}$ is further divided into Elemental Carbon (EC), Organic Carbon (OC), SO_4^{2-} and mineral ash. Ship emissions were provided in two vertical layers

285 with emissions below and above 36 m height in order to differentiate between emissions from large ships with high stacks and the smaller vessels with lower stack heights (Fig. 2). The stack release heights were attributed to the corresponding mid-points of model layers in TAPM, 15 m for the emissions below 36 m height and layer 36 m for emission above 36 m.

9

2.2.2 Road traffic emissions

290   The road traffic emissions were calculated from traffic activity data and emission factors. The basic set of emission factors from road vehicles was extracted from HBEFA v. 3.2 (HandBook Emission FActors for Road Transport, Rexeis et al., 2013). HBEFA comprehends emission factors for different classes of road vehicles based on type of vehicle (e.g. motorcycles, light-duty, heavy-duty vehicles), technology or fuel (e.g. petrol, diesel, hybrid) and emission standard (pre-Euro–Euro 6). For each of those also a number of road categories and driving patterns that affect emissions are specified within the vehicle sub-

295   segments. These emission factors include also emissions of wear particles as well as evaporative VOC emissions. The emission factors for light-duty and heavy-duty vehicles and busses in Gothenburg were calculated using the Swedish national database on car fleet composition and national, vehicle-type specific, activity data in 2012. Road traffic emissions were finally calculated using traffic activity data for Gothenburg (vehicle kilometres for light duty vehicles plus motorcycles, heavy duty vehicles and busses on road links with specified type, speed and congestion hours) from the database of the Environmental Administration,

300   City of Gothenburg (Miljöförvatningen), and corresponding emission factors calculated in the HBEFA database. These data were applied as line emission sources in the model. Resuspension of the road dust is not covered in the model.

2.2.3 Other emissions

Ten large point sources from industrial processes are present in the city-scale model domain, these are all fugitive emissions

305   from fuel handling and refineries. For technical reasons these were considered as area sources in the model with release heights corresponding to the stack heights allocated to these sources. The emission factors from these industrial sources were obtained from Swedish Environmental Emission Data (SMED 2015) for 2012.

Emissions from the following sectors were geographically distributed on 1 km × 1 km grid and assigned with emission height:

310   'Manufacture of solid fuels and other energy industries', 'Combustion in industry for energy purposes', 'Stationary combustion in agriculture/forestry/fisheries', 'Energy and heat production (commercial/institutional)', 'Residential plants (boilers), domestic heating, working and off-road machinery', 'Use of paints and chemical products in households and enterprises', 'Agriculture, waste and sewage', as well as 'Other transports' (the landing and take-off emissions from aviation, trains and military). They stem also from the SMED database and were obtained gridded on the 1 km × 1 km grid from SMHI (Swedish

315   Meteorological and Hydrological Institute). These emissions were applied as gridded sources in the model.

The local emissions of NO_x, SO_2, PM_{10} and VOC from the above-mentioned sectors in the model domain are shown in Fig. 3. The local shipping was the dominant emission source of SO_2 contributing with 61 % to the total SO_2 emissions (502 ton/year) in the model domain. Further, local shipping contributed with 41 %, of the NO_x emissions in the model domain, which was

320   comparable to contribution from the road traffic (47 %), to total NO_x emissions of 5072 ton/year. However, the road traffic was the major contributor for PM_{10} in the model domain (45 % of 357 ton/year), while the local shipping and industry

contributed with approximately 25% each. For VOC (7457 ton/year), about 92 % of emissions were released from the industrial sector and only 0.3 % from the local shipping.

2.3 Design of model simulations

325 Several model simulations were performed to investigate the influence of shipping within the city domain and influence of the regional shipping outside the city on air pollution in 2012:

(1) A simulation including complete emission inventory both in the city-scale simulation and in the CMAQ simulation supplying the chemical boundary conditions: "Base scenario";

(2) A simulation excluding the local shipping in the TAPM city domain but including regional shipping chemical 330 boundary conditions in the CMAQ simulation: "No local shipping scenario" and;

(3) A simulation excluding both local shipping in the TAPM city domain and shipping in the chemical boundary conditions in the CMAQ simulation: "No local and regional shipping scenario".

In addition, three sensitivity studies were performed within this study:

335 (1). "No NMVOC from local shipping" had the same emission input as the "Base scenario", but without NMVOC from local shipping emissions. The difference between "Base" and "No NMVOC from local shipping" was used to investigate the impact of VOC emissions from local shipping, which is often neglected in the emission inventories due to its small proportion and as these has only recently been included in the STEAM model;

(2). "Primary PM from local shipping" had the same emission input as the "Base scenario", but for the local shipping only 340 the primary PM emissions as calculated by the STEAM model were included, all emissions of the gaseous species were excluded preventing formation of the secondary PM from local shipping. The difference between "Base scenario" and "Primary PM from local shipping" reflects the formation of secondary PM from SO_2, NO_x and VOC emitted by the local shipping;

(3). "No road traffic" had the same emissions as the "Base scenario", but without road traffic emissions. It was used to 345 compare the contributions of shipping emissions as well as the health impact of shipping with emissions from the city traffic.

2.4 Model evaluation

Model evaluations were carried out for both meteorological and air pollution parameters. The simulated meteorological parameters (temperature, relative humidity, wind fields and precipitation) were evaluated with measurements at four stations: 350 Femman (57.70° N, 11.97° E, 30 m a.s.l.), Göteborg A (57.72° N, 11.99° E, 3 m a.s.l.), Vinga A (57.63° N, 11.60° E, 18 m a.s.l.) and Landvetter (57.68° N, 12.29° E, 154 m a.s.l.). The urban background site Femman is located on a rooftop in the city center and the local meteorological variables as well as the air quality data are continuously measured by the Environmental Administration in Gothenburg (Miljöförvaltningen), while the other three meteorological stations are driven by SMHI. For the

air pollution evaluation, Femman, Haga and Mölndal were included. Haga is located in a one-sided street canyon in central Gothenburg with a park to the east of the station. Mölndal is located in southern part of Gothenburg on a rooftop about 30 m above ground and corresponds to a traffic station. NO_2 is measured by a reference chemiluminescent method at Femman and Haga and by Differential Optical Absorption Spectrometry (DOAS) method at Mölndal. PM_{10} mass concentrations are measured by TEOM (Tapered Element Oscillating Microbalance, model 1400ab) instrument at all three stations. Ozone instrument at Femman was Teledyne (model T400) and at Mölndal a DOAS from OPSIS. Hourly averaged air quality data for NO_2, PM_{10}, $PM_{2.5}$ and O_3 at the three air quality stations were used to evaluate the model performance.

The FAIRMODE DELTA Tool version 5.4 was used for the evaluation of the model results for the city of Gothenburg. DELTA Tool is an IDL (Interface Definition Language)-based statistical evaluation software which allows to perform diagnostics of air quality and meteorological model performance (Thunis et al., 2012, Pernigotti et al., 2014). The tool focuses on the air pollutants regulated in the Air Quality Directive 2008 (AQD 2008) and calculates statistical performance indicators such as Mean, Exceed, Normalized Mean Bias (NMB), Normalized Mean Standard Deviation (NMSD) and High Percentile (H_{perc}) (see section S1 in the Supplement). Moreover, a performance criteria can be calculated, which is combining the statistical performance indicators with fixed parameters to evaluate whether the model results have reached a sufficient level of quality for a given policy support application (Pernigotti et al. 2014). According to the DELTA tool, the capability of a model to reproduce measured concentrations is good when more than 90 % of the stations fulfil the performance criteria. We applied the Delta Tool to concentrations of NO_2, $PM_{2.5}$, PM_{10} and O_3 measured at the available urban background sites and road traffic sites, compared them with concentrations calculated by our model system and calculated both, statistical performance indicators and the model performance criteria.

2.5 Health impact assessment

The health impacts of exposure of population in Gothenburg to shipping-related air pollutants were assessed with the ALPHA-RiskPoll (ARP) methodology (Holland et al., 2013) providing for calculation of a wide range of air-pollutant specific health effects based on the population weighted concentrations, national population statistics on age distribution of population, mortality and morbidity data and effect-specific exposure-response relationships. The methodology has been developed and used for quantification and assessments of the benefits of air pollution controls in Europe for the UN/ECE Convention on Long Range Transport of Air Pollution and is based on work for the Clean Air For Europe (CAFÉ) Program and on EU project Modelling of Air Pollution and Climate Strategies (EC4MACS). Following the WHO recommendations (WHO 2013a) and the Clean Air for Europe (CAFÉ) cost-benefit analysis methodology for assessment of health impacts of air pollutants, impacts of exposure to $PM_{2.5}$, ozone and NO_2 have been considered in the analysis. The exposure to these three pollutants is considered most harmful by the World Health Organization (WHO, 2013b). In this study only the most serious impacts, i.e. losses of lives, are presented, taking into account impacts of long-term exposure to $PM_{2.5}$ and short-term exposures to ozone and NO_2, i.e. the impacts marked A* in the HARPIE study (WHO 2013a). For ozone the indicator SOMO35 is used, representing the 8-hourly

12

mean ozone concentrations accumulated dose above a threshold of 35 ppb during a year. The health impacts of some pollutants are correlated and that is why the premature deaths attributed to each pollutant cannot simply be added up. In particular, it has been estimated that adding premature deaths attributed to $PM_{2.5}$ to those attributed to NO_2 could result in double counting of around 30 % (WHO 2013a). The health impacts calculated with the ARP model are presented as premature deaths and YOLLs per year, using the ER function of the model, i.e. 1.0062 (95 % CI 1.004–1.008) per µg/m^3 (WHO, 2013a).

The concentrations fields of $PM_{2.5}$, O_3 and NO_2 were calculated by the coupled high resolution (250 m × 250 m) modeling system, as described above. Annual means and SOMO35 were calculated from hourly concentrations for each grid. Population data on 1 km × 1 km resolution were obtained from Statistics Sweden (SCB) for 2015 with a population of 572 779 in the city of Gothenburg. As there are no significant changes in population density between 2012 and 2015, the population data for 2015 were used. Population-weighted average concentrations (PWC) for the model domain were calculated multiplying the modelled annual mean concentration of the pollutant on each grid-cell by the population in the same grid-cell as weight for the modelled concentration.

To calculate the health risks, further information needed is the ERF and the baseline health statistics including the life expectancies, the death rates and morbidity data for estimating the impacts on mortality and morbidity. To estimate YOLLs, the age at which the premature deaths occurred should also be considered. In the ARP model, the ERFs used are those from WHO (2013a): 6.2 % (95 % confidence interval 4.0–8.3 %) relative risk increase per 10 µg/m^3 increased exposure for the $PM_{2.5}$ exposure, 0.29 % (95 % confidence interval 0.14–0.43 %) relative risk increase per 10 µg/m^3 increased exposure for the ozone exposure and 0.27 % (95 % confidence interval 0.16–0.38 %) relative risk increase per 10 µg/m^3 increased exposure for the NO_2 exposure. ARP uses linear ERFs, recognizing the limited range of pollutant exposures in Europe. The YOLLs are calculated per year, applying the relative risk within national life tables. This is done through relation between the life years lost per 100 000 population per unit $PM_{2.5}$ concentration and the life expectancy of the population developed by Miller et al. (2003) based on analysis of the life tables. The premature deaths are calculated using the ERF for all-cause mortality and the total national mortality rates. This methodology is justified for European countries with health status and proportion of natural mortality of population corresponding to population studied in the epidemiological studies which brought forward these ERFs. For regions with high concentration levels of $PM_{2.5}$ the HIA studies need to use different form of ERFs and for populations with different health status and proportion of natural mortality comparing to the US and Western Europe, cause-specific rather than all-cause mortalities need to be used. In this study the analysis was made separately for the population exposure related to the different pollutants from local and regional shipping.

3 Results and discussion

3.1 Model evaluation

The model evaluation was conducted for both meteorology and air pollution in the inner-most model domain. The comparison between hourly measured and modelled local meteorological parameters (temperature, relative humidity, total solar radiation, wind speed, wind direction and precipitation) shows high correlation and low bias: averaged over all available stations, temperature and wind speed are slightly underestimated with -0.46°C and -0.18 m/s, respectively. A detailed analysis can be found in Table S1 in the Supplement. The application of ERA5 datasets in the model shows significant improvements from the default reanalysis datasets. Nevertheless, the predictions of the meteorological parameters such as wind fields flow get better with wind field assimilation, for more detail see Ramacher (2018). For example, the differences between observed and simulated wind rose at Femman in January and July indicate a good model capability to reproduce local wind field except for missing about 30% of low wind speeds (0–2.5 m s^{-1}) from the north (Fig. 4), which may introduce some underestimations in high pollutant concentrations at ground due to accumulation in the boundary layer. Nevertheless, the total frequency of northerly winds at Femman station is low in January (8–17%) and very low in July (1–8%).

The evaluation of ambient pollutants was conducted through the major statistical parameters (Table S2 in the Supplement). At urban background site Femman, the estimation of NO_2, PM_{10} and $PM_{2.5}$ concentrations were satisfactory in summer with lower bias (-0,16 µg/m³), however the model tended to underestimate NO_2, PM_{10} and $PM_{2.5}$ concentrations in winter (-15,35 µg/m³). O_3 evaluation was carried out at station Femman and Möldal, and underestimation of daily maximum of the 8-hour means was also detected, which could be caused by low resolution of local NO sources and hence more smoothed titration of ozone. The summary statistics according to the FAIRMODE model evaluation tool shows that less than 90% of daily PM_{10} concentrations at road site Haga fulfill the performance criteria for the statistic indicator H_{perc} (Fig. 5). The indicator H_{perc} indicates the model capability to reproduce extreme events, represented by selected high percentile for modelled and observed values. A detailed evaluation of simulated concentrations in form of scatter plots of modeled versus measured daily concentrations can be found in Fig. S1 in the Supplement.

The underestimation of NO_2 and PM_{10} especially at road sites demonstrate impact of too coarse spatial resolution (250 m × 250 m) not capturing high concentrations at street level, possible missing or insufficient cover of local emissions like resuspension particulate matters from traffic sources, or incomplete chemical reactions in the model etc. As pointed out by Karl (2019b), recent nested model approaches have not resolved the details in the emission processing and near-field dispersion at the street and neighborhood level. However, shipping emissions are, when reaching the exposed population, more dispersed and the 250×250 m^2 grid resolution should be sufficient to assess their impact. Nevertheless, the other statistic indicators

14

(Mean, exceedances, Normalized Mean Bias, Normalized Mean Standard Deviation, Correlation coefficient, etc.) of model performance in Fig. 5 show a satisfactory performance of the used city-scale model for Gothenburg.

3.2 Impact of ship emissions on local air quality

3.2.1 SO$_2$

The study was performed for year 2012 conditions, when the sulfur content in marine fuels was limited to 1 % in the region and 0.1 % for ships at berth. With these fuel Sulphur limits the local shipping is still the dominant local emission source of SO$_2$ (60 %) and influences the area around main shipping routes and city ports (Fig. 6). The calculated annual mean concentration of SO$_2$ from all sources in the model domain is 0.4 ppb and the local shipping contributes with 0.05 ppb (13 %) on the model-domain average and between 0.3 ppb, up to 0.6 ppb in a wide area around the main shipping routes and ports. The impacts were higher in summer than in winter (Fig. S2 in the Supplement), being result of higher shipping emission in summer as well as of differences in meteorological situation. The highest SO$_2$ contributions (maximum 0.7 ppb on annual mean and 0.8 ppb in summer) were found around the major ports: Älvsborgshamnen, Skandiahamnen, Skarvikshamnen, Ryahamnen, Lindholmshamnen, and Frihamnen in the northern bank of the Göta älv (Fig. 6d). In addition, two busy ferry terminals located on the southern bank of the Göta älv can contribute to the high SO$_2$ concentrations on the opposite river side due to the dominant south-westerly winds. The regional ship emissions outside the model domain contribute with additional 0.06 ppb (15 %) on the model-domain average. In difference from the local-shipping, this contribution is distributed rather evenly over the model domain.

The modelled SO$_2$ concentrations in Gothenburg are relatively low and Fig. 6 shows highest concentrations around the city ports as well as around industrial areas north of Göta älv. The dominated south-westerly winds transport emissions from the shipping routes and port areas farther inlands to the north. Eriksberg, located on the north waterfront of Göta älv, is today a modern residential and commercial center built in place of an old dockyard area. We have selected this place to study relative impact of shipping in more detail. The shipping-related monthly contributions to SO$_2$ concentrations at Eriksberg were 47% on average and over 60% on June-August. Figure S3 in the supplement shows the modelled monthly mean relative contributions at Eriksberg.

3.2.2 NO$_2$

NO$_x$ is mainly emitted as nitrogen oxide (NO), in the STEAM model the NO$_2$/NO$_x$ ratio is 5%. In atmosphere NO is quickly converted to NO$_2$ in reaction with ozone, so further from the source the atmospheric NO$_x$ is dominated by NO$_2$, approaching a photo-stationary state driven by the NO+O$_3$ reaction and NO$_2$ photolysis. Maps of modelled annual mean atmospheric concentrations of NO$_2$ over the Gothenburg area are shown in Fig. 7. The annual mean concentration of NO$_2$ in the Base simulation is 3.7 ppb as the model-domain average (Fig. 7a), and the model-domain mean contribution from local shipping to

15

the annual mean concentrations is 0.5 ppb (14%) and up to 3.3 ppb in areas with high contribution (Fig. 7b). The relative contribution of local shipping to the NO_2 concentrations in the model domain in Gothenburg is comparable with 11% in Riga (Latvia), 16% in Gdańsk-Gdynia (Poland) and 22% in Rostock (Germany) in 2012 (Ramacher et al. 2019). The calculated model-domain mean contribution to NO_2 concentrations from regional shipping is 1.0 ppb (26%), and up to 1.2 ppb in most heavily impacted areas (Fig. 7c), which is larger than local shipping contributions. The total shipping-related relative contribution in Gothenburg to the NO_2 annual averaged grid mean in the model domain is 40%. In summer the contribution reaches 49% (17% from local shipping + 32% from regional shipping) to the summer average NO_2 concentration in the model domain and influenced areas expands to further inland. This is result of 20% higher summer emissions comparing to winter, different photochemical state as well as different local meteorological conditions (Fig. S4 in the Supplement).

Nearly 90% of NO_x emissions in Gothenburg are from road traffic (47%) and local shipping (41%). Impact of the local shipping is concentrated in areas inside the harbor along the Göta älv and decreases with growing distance to the port areas. Fig. 8 presents impacts of the local and regional shipping, as well as of the road traffic and all other anthropogenic sources (including NO_2 coming from the model domain boundary) on monthly levels at Eriksberg. The modelled annual mean NO_2 concentration from all sources is 7.5 ppb at Eriksberg, in which 2.5 ppb (33%) originates from local shipping, 1.0 ppb (13%) from regional shipping and 2.1 ppb (28%) from road traffic. The maximum relative contributions from local shipping and regional shipping to the monthly mean concentrations reach 43% in July and 16% in June. The monthly average contributions from the local and regional shipping together are larger than or comparable to the contributions from the road traffic in all months. Even though the road traffic is the major contributor to the NO_2 concentrations in urban environment, the local ship emissions are of major concern, especially in areas close to the city ports.

3.2.3 O_3

O_3 is formed in photocatalytic cycles involving NO_x, ozone and hydrocarbons, through the photolysis of NO_2 in sunlight. The same cycle involves also titration of ozone by the reaction with NO forming the NO_2. Maps of modelled atmospheric concentrations of ozone over the Gothenburg area in 2012 are shown in Fig. 9, with focus on summer months (JJA). The regional background concentration of ozone at regional background station Råö close to Gothenburg area is 37 ppb in the summer of 2012. Modelled summer ozone levels in the model domain are in the 15–30 ppb range (domain average is 28.6 ppb) (Fig. 9a). Since NO_x is mainly emitted as NO, the emissions from local shipping cause local reduction of ozone concentrations by 0.5 ppb (~2 %) in the main shipping routes and port areas due to the titration of O_3 by NO (Fig. 9b). The O_3 depletion along the north riverbank of the Göta älv is 4 ppb (~14%) in maximum due to the local shipping with both NO_x and NMVOC emissions (Fig. 9b), while regional shipping emissions increase the ozone concentrations by 1 ppb over the land. This ozone increase can be compared to 4–6 ppb increase caused by the shipping emissions over the remote ocean as a result of large-scale summer ozone production found by Huszar et al. (2010, Fig. 9c).

16

In the local STEAM inventory, the non-methane volatile organic compounds (NMVOC) from shipping were introduced. These NMVOC serve as precursors of O_3 and enhance photochemical ozone production. TAPM model uses concept of VOC reactivity instead of individual NMVOCs, producing pool of peroxy radicals which take part in the ozone-production photocatalytic cycle. A sensitivity run was performed to study the impact of VOC emissions from the local shipping on ozone concentrations in the city by excluding the local shipping VOC emissions from the simulation. Fig. 9d shows the impact of the VOC emissions: the O_3 concentrations increase by up to 2 ppb (~7 %) along the main shipping routes and the port areas, which means that the titration effects of NO_x emissions from local shipping on the ozone concentrations was 6 ppb in maximum when VOC emissions were excluded, comparing to 4 ppb in the Base simulation. Sensitivity of ozone formation to VOC emissions also clearly indicates that the city centre is most often in VOC-limited regime. Further details of impact of the shipping emissions on ozone formation are illustrated in Figure S5 in the Supplement, showing summer ozone formation from regional and local shipping as well as from the local shipping VOC emissions at Eriksberg. At this location the local shipping emissions lead almost always to ozone depletion. On contrary, VOC emissions from local shipping cause the increase of ozone concentrations, confirming that the location is in a VOC-limited photochemical regime. The regional shipping tends to increase the local ozone concentrations in most of days (78 days under June–August). Inspecting details of the diurnal variation of ozone contributions (Figure S5b-d), one can see that during the rare occasions without ozone depletion by the local shipping, there is a small ozone formation from the local shipping emissions and no ozone formation from the local shipping VOC emission, indicating presence of NOx-limited regime (Fig. S5b), while during most of the studied days the local shipping emissions have an ozone depletion effect at daytime while the local shipping VOC emission have ozone formation effect peaking in the morning and sometimes also in the afternoon (Fig. S5c). The regional shipping increases the ozone concentrations in all three depicted cases, showing maxima in the afternoon.

3.2.4 Particulate matter

Particulate matter includes primary, directly emitted particles and secondary particulate matter formed upon further processing of emissions in the atmosphere. At the urban background site Femman, close to the city harbour, the measured annual mean $PM_{2.5}$ concentration was 7.9 µg m^{-3} in 2012. The calculated annual mean $PM_{2.5}$ in the Base simulation is 4 µg m^{-3} as the model domain average (Fig. 10a). The local ship emissions contributed with 0.1 µg m^{-3} (3 %) to the annual mean as the model-domain average (Fig. 10b), which had same relative contribution as 3% in Gdansk-Gdynia and higher than 1% in Rostock and Riga in 2012 (Ramacher et al., 2019). Regional shipping was under 2012 conditions a larger contributor to the local $PM_{2.5}$ than the local shipping with annual mean average contribution of 0.4 µg m^{-3} (11 %) (Fig. 10c). The total ship-related relative contribution to the annual averaged $PM_{2.5}$ concentrations in model domain was 14 %, and reached in summer to 27 % (4 % from local shipping + 23 % from regional shipping) to the summer averaged $PM_{2.5}$ concentrations in model domain (Fig. S6 in Supplement. At the near-harbour residential area Eriksberg the modelled annual mean $PM_{2.5}$ concentration from all sources

is 4.5 µg m^{-3}. The calculated annual mean contributions from local shipping and regional shipping are 0.2 µg m^{-3} (~4 %) and 0.4 µg m^{-3} (~9 %) respectively. The maximum monthly relative contribution from the local and regional shipping was about 29 % in July, in which 21% from regional shipping (Fig. 11). Road traffic, the largest local source of PM$_{10}$, contributed up to 5% of monthly PM$_{2.5}$ mean concentrations. The large contribution of PM$_{2.5}$ from regional shipping is agree with the character of source apportionment in Gothenburg. An early study shows that the main sources types of PM$_{2.5}$ in Gothenburg were long-range transport (LRT) (about 50 %), followed by ship emissions (20 %) and local combustion (19 %) for year 2008–2009 (Molnár et al., 2017).

The secondary aerosol formation in TAPM is heavily parameterized, however, captures the important features of the secondary particle formation, i.e. formation of sulphate and nitrate following the SO$_2$ and NO$_2$ oxidation, as well as formation of SOA as a fixed part of the degraded smog reactivity representing VOC species in the reaction scheme of TAPM (Hurley et al. 2008b). On urban scale, formation of secondary PM is usually supressed as the radical pool is depleted by the primary emissions and many urban models do not consider the secondary PM at all. Therefore, a sensitivity run was performed to investigate the role of the formation of secondary PM from local shipping on the city scale where only emissions of the primary PM were introduced, without emissions of the gas-phase pollutants from the local shipping. Modelled secondary PM concentrations from shipping were calculated as the difference between the base run and this sensitivity run. Fig. S7 in Supplement shows contributions of max. 2% of the PM related to the local shipping in Gothenburg in winter months and negligible contributions in summer. The secondary PM, mainly formed far from the sources, tends to disperse and accumulate to the east part of Gothenburg due to the prevailing wind directions.

4 Calculation of exposure and health effects from ship emissions

The contribution of emission sources to population exposure depends on the relationship between population density and air pollution levels. The areas with relatively high exposure to PM$_{2.5}$ due to local and regional shipping are city ports and areas around, especially north of the Göta älv. Figure 12 presents the population weighted annual mean concentrations of NO$_2$, PM$_{2.5}$ and SOMO35 at each model grid for the base simulation and for contributions of the local plus regional shipping, as well as for contributions of the road traffic. The spatial patterns of PM$_{2.5}$ exposure from shipping are dominated by gradients in the concentration fields around the city ports to the north of Göta älv. PM$_{2.5}$ exposure from shipping is higher than exposure from road traffic in a larger city area since regional-shipping-related PM$_{2.5}$ exposure is evenly distributed over the city (Fig. S8 in the Supplement). The sum of PWC of PM$_{2.5}$ from the local plus regional shipping is 0.51 µg m^{-3} in the model domain, to which the regional shipping contributes with 82 %, comparing to 0.22 µg m^{-3} associated to road traffic (Table 2). The total exposure to PM$_{2.5}$ is dominated by particles transported to the city with the background air. The sum of PWC of NO$_2$ from regional and local shipping was 1.65 ppb, similar to that from the road traffic (1.75 ppb), with gradients in the concentration fields north of the Göta älv. Because of the effect of local O$_3$ titration by the shipping emitted NO, the exposure to SOMO35 from shipping

was negative along the Göta älv. However, SOMO35 exposure due to regional shipping was positive with sum of PWC 70.9 ppb×h in the model domain and showed relatively high level in areas with high population density.

The PWC for these pollutants were then used in the health impact calculations and results are presented as life years lost per
580   year and loss of life expectancy (years of lifetime lost per person, YOLLs pers.$^{-1}$) for PM$_{2.5}$ and as premature deaths for ozone and NO$_2$. The estimated loss of life expectancy (YOLLs pers.$^{-1}$) due to PM$_{2.5}$ from local shipping was 0.003 while from the regional shipping it was 0.014. For comparison, impact of exposure to PM$_{2.5}$ from the road traffic was calculated to be 0.007 YOLLs pers.$^{-1}$ and to all PM$_{2.5}$ in the Base simulation to be 0.14 YOLLs pers.$^{-1}$ (Table 3). In all, shipping contributed with 12 % to the calculated health impacts from the total exposure to PM$_{2.5}$ in the city and the impact was more than 2 times larger
585   than that of the local road traffic, the regional shipping being a larger risk for human health than the local shipping (> 80 %) in Gothenburg. The exposure to ozone related to shipping emissions reduced the acute mortality by 0.4 premature deaths per year due to the NO titration effect. This effect included additional 0.03 deaths attributed to ozone formed from the regional shipping emissions (Table 3). Exposure to NO$_2$ related to shipping emissions caused additional 2.6 premature deaths year^{-1}, impact of the local shipping being similar to the regional one. This impact corresponded to 35 % of the impact of the NO$_2$
590   exposure in the Base simulation and was similar to the impact of the road traffic.

5 Assessment of uncertainties and comparison with other studies

Addressing uncertainties in human health risk assessment is a critical issue when evaluating the effects of contaminants on public health due to the complex associations between environmental exposures and health. Uncertainties are introduced with
595   the calculated pollutant concentrations, the grid resolution when assessing the population exposure, the general shape of concentration-response function and transferability problems of the function from region to region. Hammingh et al. (2012) presented an estimate of the uncertainty in the calculations of YOLLs, which may stem from the methodology used in the YOLL calculations and from the spatial resolution. To compare results of Jonsson et al. (2015) with results of this study, the YOLLs pers.$^{-1}$ from PM$_{2.5}$ exposure calculated in ARP were multiplied by the life expectancy of population above the age of
600   30, i.e. 50 years, and divided by the population in the model domain. The health impacts of PM$_{2.5}$ were also calculated using the RAINS methodology directly on the calculated PM$_{2.5}$ exposures. Results of both methods are presented, giving very similar results.

The largest uncertainties are associated with the exposure response functions (ERF) as such. In this study impacts for the mean
605   values of ERFs are presented, the 95 % confidence interval for these functions is given in the Methods chapter. The ERFs used here are those recommended in WHO (2013a), for PM$_{2.5}$ ERFs with higher values for spatial analyses of air pollution and mortality were found by project Escape for European cohorts (Beelen et al., 2014) as well as for mortalities in Los Angeles (Jerrett et al., 2005, 17 % per 10 µg m^{-3}, 95 % confidence interval 5–30 %). These ERFs are of very similar value and those of Beelen et al. (2014) were used as alternative functions for estimates of broader uncertainty limits by Barregård et al. (2019).

In ARP a linear form of ERFs is applied which is justified by a rather narrow interval of PM exposure levels in Europe. In terms of impact of the total exposure to $PM_{2.5}$ on natural mortality, the linear and log-linear form of the functions give similar results within the concentration range of 10–30 µg m^{-3}, the linear model giving slightly lower relative risks in this range and higher relative risks below and above (Ostro et. al., 2004). The PM2.5 levels found in pour study falls below 10 µg m^{-3}. For regions with high PM2.5 levels different ERF models need to be applied and for global HIA studies or studies in other regions of the world but Western Europe or North America also ERFs for cause-specific mortalities, rather than natural mortalities are usually used. There are two further important issues regarding the uncertainties associated with the ERFs. First, the air pollution represents a complex mixture and individual gases and particles are often correlated. The impacts on mortality calculated for the different pollutants therefore cannot be simply summed up. Second, the ERFs assume that all particulate matter has the same impact. There is increasing evidence of different ERFs for some compounds, primarily elemental and organic carbon (WHO 2013b).

The most robust relation between the air pollution and effects on human health is for particulate matter (WHO 2013b). In Swedish cities, also in Gothenburg, the main contribution to concentrations of $PM_{2.5}$ comes from the background air (Segersson et al., 2017; Gustafsson et al. 2018). Accurate modelling of the total concentration of particulate matter is, however, very difficult as the processes affecting them are extremely complex and many of them not well quantified. These include natural and anthropogenic emissions, formation of secondary particulate matter in complex photochemical processes as well as dry and wet deposition processes that need to be described on the whole range of relevant geographical and time scales. Many regional- and global-scale models tend to underestimate the simulated $PM_{2.5}$ concentrations, especially in summer, when formation of secondary PM is stronger due to the high photochemical activity and the impact of primary PM is lower due to the more intensive mixing and smaller anthropogenic emissions of primary PM in summer (Karl et al., 2019a). Also, the modelled PM concentrations used as the boundary conditions in this study showed underestimates of $PM_{2.5}$ by 60 % and 17 %, on summer average and on annual average, respectively (Karl et al., 2019a). Two studies addressing impacts of shipping on air pollution in Gothenburg (Segersson et al., 2017; Repka et al., 2019) assessed the total concentration levels and contribution of shipping to these, none of them are, however, calculated for year 2012 assessed in this study. Segersson et al. (2017) shows annual mean background $PM_{2.5}$ concentrations for year 2011 of about 5 µg m^{-3} for Gothenburg, reaching concentrations > 8 µg m^{-3} in polluted parts of the city. An annual mean concentration map presented in Repka et al. (2019) for year 2016 shows similar concentration levels with background concentrations of about 6 µg m^{-3} and maximum concentrations > 8 µg m^{-3}. Both studies used PM_{10} monitoring data at the urban background station 'Femman' to inversely derive the boundary conditions for $PM_{2.5}$. Jonson et al. (2015 and 2019) studied impacts of the Baltic Sea and North Sea shipping with the EMEP model for year 2010 and 2016 and found in both cases annual mean concentration levels at the Swedish West coast about 4–5 µg m^{-3}. This concentration should correspond to the background levels of the city-scale simulations and year 2016. Jonson et al. (2019) also compared the modelled concentrations with background measurements from the station Råö, situated 20 km south of the city, and found a model underestimation of 0.7 ppb for the annual mean. The concentration levels of $PM_{2.5}$ found

in this study were lower than in Segersson et al. (2017) and Repka et al. (2019), but they agree reasonably well with Jonson et al., 2015 and 2019. Segersson et al. (2017) addressed health effects of $PM_{2.5}$, PM_{10} and black carbon in three Swedish cities, among them Gothenburg using gaussian model SIMAIR. The population weighted exposure to $PM_{2.5}$ for Gothenburg was calculated to 6.5 µg m^{-3}, which was associated with c.a. 150–290 premature deaths from exposure to $PM_{2.5}$. The lower premature death number in Segersson et al. (2017) comes from calculations using the same ERF as in this study while the higher number uses the ERF presented by Jerrett et al. (2005) for $PM_{2.5}$ from the city sources. The values can be compared to the population weighted exposure to $PM_{2.5}$ of 4.1 µg m^{-3}, associated to c.a. 140 premature deaths found in this study. Jonson et al. (2015) calculated impact of shipping emissions in the Baltic Sea and the North Sea using the EMEP model and a map presenting geographical distribution of life expectancy loss shows approximately 0.2 YOLLs pers.$^{-1}$ around the West coast of Sweden. This agrees reasonably well with our estimate of 0.18 YOLLs pers.$^{-1}$ in Gothenburg.

It is important to bear the uncertainties in total concentrations of PM and other air pollutants in mind when assessing the relative contribution of shipping to the overall impact of air pollution. Assessments of impacts of selected anthropogenic sources are, however, associated with smaller uncertainties compared to the impact of the total concentrations as some large uncertainties, e.g. those regarding the natural and agriculture sources, cancel out. The study of Segersson et al. (2017) found contribution of shipping to the population weighted annual $PM_{2.5}$ concentration to be 0.04 µg m^{-3} and contribution of the road traffic exhaust emissions to be 0.27 µg m^{-3} which can be compared to 0.09 µg m^{-3} from shipping and 0.22 µg m^{-3} from road traffic found in this study, however, bearing in mind that the studies assessed two different years.

6 Conclusions

The impact of local and regional ship emissions on in the city of Gothenburg was investigated by a multi-model system for the year 2012. The model evaluation against monitoring data demonstrated fairly good agreement in meteorological parameters and acceptable estimation of hourly air pollutant concentrations.

The city-scale model simulations with and without local and regional shipping in the emission inventory revealed that impacts from shipping on air quality in Gothenburg were substantial. The calculated contribution from local shipping to NO_2 was 0.5 ppb on annual average, representing 14 % of calculated annual mean NO_2 concentration. Including contribution from regional shipping in the North Sea and the Baltic Sea, the total shipping contribution reached 1.5 ppb representing 41 % of calculated NO_2 concentrations. The contribution from regional and local shipping was higher than that from road traffic around the area of the city ports. In an analysis of exposure from different sources using population weighted concentrations, the contribution of regional and local shipping was similar to that of the road traffic in the city.

675   The model results of ozone concentrations have shown that titration by NO dominated the overall impact of local shipping on ozone concentration levels in Gothenburg. The maximum impact from local NO_x and NMVOC emissions on summer seasonal mean ozone concentration was calculated to -4 ppb (~14 %). The negative effect of solely NO_x emissions from local shipping on the ozone concentrations was up to -6 ppb (~21 %), net negative even in the summer, when photochemical activity and potential for ozone formation are high. The emissions of NMVOC from local shipping as such increased the ozone formation

680   in the city with the highest contribution of 2 ppb (~ 7%) as seasonal summer mean. In terms of urban air quality control, reduction in anthropogenic NMVOC could result in a significantly greater decrease in O_3 relative to the same reduction in NO_x (Karl, 2019b).

The simulated emissions from local and regional shipping contributed 0.5 µg m^{-3} on model/domain average and at highest 1.1

685   µg m^{-3} to the annual mean concentration of $PM_{2.5}$. Regional shipping is a larger contributor than local shipping to local $PM_{2.5}$ concentrations, corresponding to 11 % of the local $PM_{2.5}$ concentrations on average. Also its contribution to the PWC was higher, contributing with 0.4 µg m^{-3} (10 % of the total PWC for $PM_{2.5}$). Contribution from the local shipping was 0.1 µg m^{-3} (2 % of the total).

690   The calculated health impacts have shown the most serious effects from shipping in Gothenburg to be associated with exposure to $PM_{2.5}$. Local and regional shipping together reduce life expectancy by 0.015 years per person, of which more than 80 % are associated with the regional shipping in the North and the Baltic Sea. The shipping impact is more than twice as high as the modelled impact of $PM_{2.5}$ associated with the local road traffic. Impacts from exposure to NO_2 and ozone were calculated in terms of premature deaths per year and 2.6 additional cases year^{-1} were calculated for exposure to NO_2, regional and local

695   shipping contributing with 59 % and 41 % respectively. Impacts from exposure to ozone were of opposite magnitude. The decrease of ozone due to the NO titration reduced the calculated mortalities by 0.4 cases year^{-1}. The impact of the exposure to $PM_{2.5}$ from shipping calculated as premature deaths was 18 cases year^{-1}. The implementation of the more stringent SECA regulations on FSC in year 2015 is not likely to have changed impacts from NO_2 and ozone. According to the study of Jonson et al. (2019), approximately 35 % reduction of the impact from the regional shipping contribution to $PM_{2.5}$ could be expected

700   around Gothenburg while a much smaller change can be expected in emission from the local shipping since hotelling and inland shipping already use a fuel with 0.1 % FSC in the model. This would mean similar reductions of the impacts related to $PM_{2.5}$ in the city of Gothenburg. Impact of the global cap of 0.5 % for FSC which entered into force the 1st of January 2020 will not have any significant impact on further reduction of shipping-related air pollution in Gothenburg comparing to situation after 2015. Global study of Sofiev at al. (2018) shows that around the Swedish West coast decrease of $PM_{2.5}$ due to the global

705   cap would be below 1%. The more serious health effects induced by regional shipping indicate that close cooperation across governance levels is required to effectively reduce the air pollution in the city.

Impacts of the local shipping emissions on air quality and human health are further discussed in part II paper (Ramacher et al., 2019, the Part II paper), presenting study of several future shipping scenarios for year 2040 adopting changes in shipping
710 emissions due to changes in ship traffic volumes, legislation on emissions of air pollutants at sea, on energy effectivization as well as introduction of shore side electricity in shipping.

This article is part of the special issue "Shipping and the Environment 2017"

Code availability

715 The TAPM model is a commercial software available at CSIRO, Australia (www.csiro.au). STEAM model is intellectual property of the Finnish Meteorological Institute and is not publicly available. ARP is commercial software available from arirabl.com.

Data availability

The model output data are available upon request from the corresponding authors

720 **Author contribution**

LT, MOPR, JM and VM designed the model simulations. LJ and JPJ calculated ship emissions with the STEAM model and contributed with text about the shipping emissions, LT prepared ship emission files for the model simulations. LT, MG and JM prepared emission data from other sources. MK and AA prepared data from the regional-scale simulation used for the boundary conditions and MK contributed with text about these simulations. LT and MOPR prepared the model set-up and
725 other input data, performed the model simulations and evaluated the model results. LT calculated exposures and JM and KY calculated the health impacts. LT and JM wrote the major part of the text with assistance from MOPR and VM.

Competing interests

JM is associated editor of the special issue Shipping and Environment.

References

Amann. M., Cofala, J., Heyes, C., Klimont, Z., Mechler, R., Posch, M., and Schöpp, W.: Documentation of the model approach prepared for the RAINS peer review 2004, Interim Report IR-04-075, 2004.

Andersson, C., Bergström, R., and Johansson, C.: Population exposure and mortality due to regional background PM in Europe – Long-term simulations of source region and shipping contributions. Atmos. Environ., 43, 3614–3620, 2009.

Åström, S., Yaramenka, K., Winnes, H., Fridell, E., Holland, M.: The costs and benefits of a nitrogen emission control area in the Baltic and North Seas. Transportation Res. D, 59, 223-236, 2018.

Aulinger, A., Matthias, V., Zeretzke, M., Bieser, J., Quante, M., and Backes, A.: The impact of shipping emissions on air pollution in the greater North Sea region – Part 1: Current emissions and concentrations, Atmos. Chem. Phys., 16, 739–758, doi:10.5194/acp-16-739-2016, 2016.

Azzi, M., Johnson, G.M., and Cope, M.: An introduction to the generic reaction set photochemical smog mechanism, Proceedings of the 11th International Clean Air and Environment Conference, Brisbane, 1992, Clean Air Society of Australia & New Zealand, 1992.

Barregård, L., Molnár, P., Jonson, J-E., and Stockfelt, L.: Impact on population health of Baltic shipping Emissions, Int. J. Environ. Res. Public Health, 16, 1954, 2019.

Beelen, R., Raaschou-Nielsen, O., Stafoggia, M., Andersen, Z.J., Weinmayr, G., Hoffmann, B., Wolf, K., Samoli, E., Fischer, P., Nieuwenhuijsen, M., Vineis, P., Xun, W.W., Katsouyanni, K., Dimakopoulou, K., Oudin, A., Forsberg, B., Modig, L., Havulinna, A.S., Lanki, T., Turunen, A., Oftedal, B., Nystad, W., Nafstad, P., De Faire, U., Pedersen, N.L., Östenson, C.G., Fratiglioni, L., Penell, J., Korek, M., Pershagen, G., Eriksen, K.T., Overvad, K., Ellermann, T., Eeftens, M., Peeters, P.H., Meliefste, K.,Wang, M., Bueno-De-Mesquita, B., Sugiri, D., Krämer, U., Heinrich, J., De Hoogh, K., Key, T., Peters, A., Hampel, R., Concin, H., Nagel, G., Ineichen, A., Schaffner, E., Probst-Hensch, N., Künzli, N., Schindler, C., Schikowski, T., Adam, M., Phuleria, H., Vilier, A., Clavel-Chapelon, F., Declercq, C., Grioni, S., Krogh, V., Tsai, M.Y., Ricceri, F., Sacerdote, C., Galassi, C., Migliore, E., Ranzi, A., Cesaroni, G., Badaloni, C., Forastiere, F., Tamayo, I., Amiano, P., Dorronsoro, M., Katsoulis, M., Trichopoulou, A., Brunekreef, B., and Hoek, G.: Effects of long-term exposure to air pollution on natural-cause mortality: an analysis of 22 European cohorts within the multicentre ESCAPE project. Lancet 383, 785–795, 2014. https://doi.org/10.1016/S0140-6736(13)

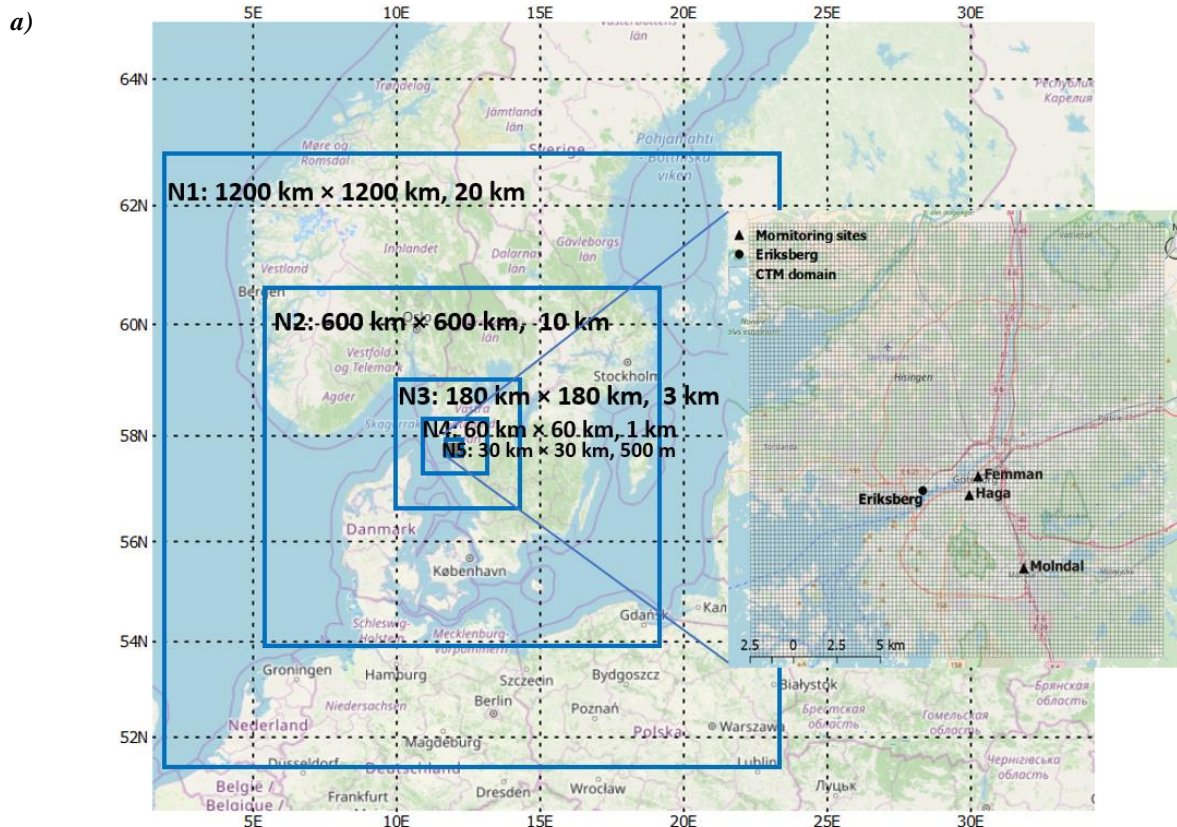765 Bieser, J., Aulinger, A., Matthias, V., Quante, M., and Builtjes, P.: SMOKE for Europe - adaptation, modification and evaluation of a comprehensive emission model for Europe, Ge-oscientific Model Development 4(1), 47–68, 2011.

Byun, D. and Ching, J.: Science Algorithms of the EPA Models-3 Community Multiscale Air Quality Modeling System, Epa/600/r-99/030, US Environmental Protection Agency, Office of Research and Development, Washington DC, 1999.

Byun, D. and Schere, K.: Review of the Governing Equations, Computational Algorithms, and Other Components of the Models-3 Community Multiscale Air Quality (CMAQ) Modeling System, Appl. Mech. Rev., 59, 51–77, 2006.

770 CEIP: WebDab – EMEP database, available at: http://www.ceip.at/emission-data-webdab/emissions-used-in-emep-models/, last access: 7 October 2018.

Cofala, J., Amann, M., Heyes, C., Wagner, F., Klimont, Z., Posch, M., Schöpp, W., Tarasson L, Jonson, J.E., Whall, C., and Stavrakaki, A.: Analysis of policy measures to reduce ship emissions in the context of the revision of the National Emissions Ceilings Directive, IIASA report, No. 06-107, 2007.

775 Corbett, J.J., Fischbeck, P.S., and Pandis, S.N.: Global nitrogen and sulfur inventories for oceangoing ships, J. Geophys. Res., 104, 3457–3470, 1999.

EPER: European Pollution Emission Register, available at: https://www.eea.europa.eu/data-and-maps/data/ member-states-reporting-art-7-under-the-european-pollutant-release-and-transfer-register-e-prtr-regulation-16, last access: 7 February, 2018.

780 Eyring. V., Köhler, H.W., van Aardenne, J., and Lauer, A.: Emissions from international shipping: 1. The last 50 years. J. Geophys. Res., 110 (D17305), 2005.

Fridell, E, Haeger-Eugensson, M, Moldanova, J, Forsberg, B. and Sjöberg, K.: A modeling study of the impact on air quality and health due to the emissions from E85 and petrol fueled cars in Sweden, Atmos. Environ. 82, 1–8, 2014.

Gustafsson, M., Lindén, J., Tang, L., Forsberg, B., Orru, H., Åström, S., and Sjöberg, K.: Quantificaiton of population exposure 785 to NO_2, $PM_{2.5}$ and PM_{10} and estimated health impacts, IVL report, No. C317, 2018.

Hammingh, P., Holland, M.R., Geilenkirchen, G.P., Jonson, J.E., and Maas, R.J.M.: Assessment of the Environmental Impacts and Health Benefits of a Nitrogen Emission Control Area in the North Sea. Policy studies PBL Netherlands Environmental Assessment Agency (PBL), The Hague, p. 113. 2012.

Holland, M.R., Pye, S., and Jones, G.: EC4MACS Modelling Methodology-The ALPHA Benefit Assessment Model, European 790 Consortium for Modelling of Air Pollution and Climate Strategies – EC4MACS, 2013.

Hurley, P., Physick,W., and Luhar, A.: TAPM - a practical approach to prognostic meteorological and air pollution modelling, Environ. Modell. Softw., 20, 737–752, doi:10.1016/j.envsoft.2004.04.006, 2005.

Hurley, P.: TAPM v. 4. User Manual, CSIRO, ISBN: 978-1-921424-73-1, 2008 a.

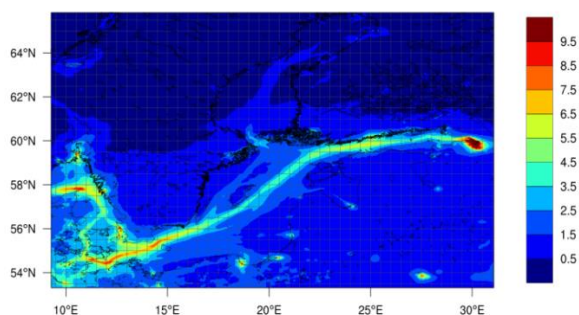Hurley, P.: TAPM v. 4. Part 1: Technical Description, CSIRO, ISBN: 978-1-921424-71-7, 2008 b.

795 Huszar, P., Cariolle, D., Paoli, R., Halenka, T., Belda, M., Schlager, H., Miksovsky, J., and Pisoft, P.: Modeling the regional impact of ship emissions on NOx and ozone levels over the Eastern Atlantic and Western Europe using ship plume parameterization, Atmospheric Chemistry and Physics, 10, 6645–6660, https://doi.org/10.5194/acp-10-6645-2010, https://www.atmos-chem-phys.net/10/6645/2010/, 2010.

Jalkanen, J.-P., Brink, A., Kalli, J., Petterson, H., Kukkonen, J., and Stipa, T.: A modelling system for the exhaust emissions
800   of marine traffic and its application in the Baltic Sea area, Atmos. Chem. Phys.9, 9209–9223, 2009.

Jalkanen, J.-P., Johansson, L., Kukkonen, J., Brink, A., Kalli, J., and Stipa, T.: Extension of an assessment model of ship traffic exhaust emissions for particulate matter and carbon monoxide, Atmos. Chem. Phys., 12, 2641–2659, doi:10.5194/acp12-2641-2012, 2012.

Jerrett, M., Burnett, R.T., Ma, R.J., Pope, C.A., Krewski, D., Newbold, K.B., Thurston, G., Shi, Y., Finkelstein, N., Calle, E.E.
805   and Thun, M. J.: Spatial analysis of air pollution and mortality in Los Angeles. Epidemiology, 16, 727–736, 2005.

Jonson, J. E., Jalkanen, J., Johansson, L., Gauss, M., and Denier van der Gon, H.: Model calculations of the effects of present and future emissions of air pollutants from shipping in the Baltic Sea and the North Sea, Atmos. Chem. Phys. 15, 783–798, 2015.

Jonson, J.E., Gauss, M., Jalkanen, J.-P., Johansson, L.: Effects of strengthening the Baltic Sea ECA regulations. Atmos. Chem.
810   Phys., 19, 13469–13487, https://doi.org/10.5194/acp-2019-13469-2019, 2019.

Jonson, J. E., Schulz, M., Emmons, L., Flemming, J., Henze, D., Sudo, K., Tronstad Lund, M., Lin, M., Benedictow, A., Koffi, B., Dentener, F., Keating, T., and Kivi, R.: The effects of intercontinental emission sources on European air pollution levels, Atmos. Chem. Phys., 18, 13655–13672, https://doi.org/10.5194/acp-18-13655-2018, 2018.

Johansson, L., Jalkanen, J.-P., Kalli, J. and Kukkonen, J.: The evolution of shipping emissions and the costs of regulation
815   changes in the northern EU area, Atmos. Chem. Phys., 13, 11375–11389, 2013.

Karl, M., Jonson, J. E., Uppstu, A., Aulinger, A., Prank, M., Jalkanen, J.-P., Johansson, L., Quante, M., and Matthias, V.: Effects of ship emissions on air quality in the Baltic Sea region simulated with three different chemistry transport models, Atmos. Chem. Phys., 19, 7019–7053, 2019a.

Karl, M., Walker, S.-E., Solberg, S., and Ramacher, M. O. P.: The Eulerian urban dispersion model EPISODE. Part II:
820   Extensions to the source dispersion and photochemistry for EPISODE-CityChem v1.2 and its application to the city of Hamburg, Geosci. Model Dev., 12, 3357–3399, 2019b.

Karl, M., Bieser, J., Geyer, B., Matthias, V., Jalkanen, J.-P., Johansson, L., and Fridell, E.: Impact of a nitrogen emission control area (NECA) on the future air quality and nitrogen deposition to seawater in the Baltic Sea region, Atmos. Chem. Phys., 19, 1721–1752, 2019c.

825   Matthias, V., Aulinger, A., Backes, A., Bieser, J., Geyer, B., Quante, M., and Zeretzke, M.: The impact of shipping emissions on air pollution in the greater North Sea region – Part 2: Scenarios for 2030, Atmos. Chem. Phys., 16, 759–776, doi:10.5194/acp-16-759-2016, 2016.

Miljöförvaltningen, 2017: Luftkvaliteten i Göteborgsområdet Årsrapport 2016 R2017:06. ISBN nr: 1401-2448

Miller B.G. and Hurley J.F. (2003). Life table methods for quantitative impact assessments in chronic mortality. J Epidemiol.
830   Community Health, 57: 200-206.

Molnár, P., Tang, L., Sjöberg, K., Wichmann, J.: Long-range transport clusters and positive matrix factorization source apportionment for investigating transboundary PM2.5 in Gothenburg, Sweden. Environmental Science: Processes & Impacts 19, 1270-1277, 2017. DOI: 10.1039/C7EM00122C.

Olivier, J. G. J., Bouwman, A. F., Berdowski, J. J. M., Veldt, C., Bloos, J. P. J., Visschedijk, A. J. H., Van der Maas, C. W.
835   M., and Zandveld, P. Y. J.: Sectoral emission inventories of greenhouse gases for 1990 on a per country basis as well as on 1◦ × 1◦, Environ. Sci. Pol., 2, 241–264, 1999.

Olstrup, H., Forsberg, B., Orru, H., Spanne, M., Nguyen, H., Molnár, P., and Johansson, C.: Trends in air pollutants and health impacts in three Swedish cities over the past three decades, Atmos. Chem. Phys., 18, 15705–15723, 2018.

Ostro, B.: Outdoor air pollution: Assessing the environmental burden of disease at national and local levels. WHO
840   Environmental Burden of Disease Series, No. 5, Geneva, WHO, 2004.

Pernigotti, D., Gerboles, M. and Thunis, P.: Modeling quality objectives in the framework of the FAIRMODE project: working document, April 2014. Available on the FAIRMODE webpage: http://fairmode.jrc.ec.europa.eu/wq1.html.

QGIS Development Team: QGIS Geographic Information System, Open Source Geospatial Foundation Project, 2017. Available online: https://www.qgis.org/en/site/# (accessed on 26 February 2018).

845   Pope, C.A., Burnett, R.T., Thun, M.J., Calle, E.E., Krewski, D., Ito, K., Thurston, G.D.: Lung cancer, cardiopulmonary mortality, and long-term exposure to fine particulate air pollution. Journal of the American Medical Association 287, 1137–1141, 2002.

Ramacher, M.O.P.: Performance and evaluation of local scale wind flow fields for urban air pollution modeling with the coupled prognostic model TAPM driven by ERA5 climate reanalysis data, Geophys. Res. Abstr, 20, EGU2018-8112, 2018.

850   Repka, S., Mellqvist, J., Borkowski, T., Jalkanen, J.-P., Jonson, J. E., Barregard, L., Olaniyi, E., Prause, G. K., Gauss, M., Walden, J., Svensson, E., Genikhovich, E., Rumyantzev, D., Boyesen, J., Wenske, C., de Carvalho, T. P., Lähteenmäki-Uutela, A., Johansson, L., Conde, V., Erkkilä-Välimäki, A., Yliskylä-Peuralahti, J., Saarnio, K., Bakhtov, A., Tochanskaya, S., Bosch, M., Haukioja, T., Törrönen, J., Karppinen, A., Beecken, J., Alhosalo, M., Myskow, J., Kowalak, P., Bäck, E., Nguyen, H., Molnar, P., Stockfelt, L., Atari, S., Bakkar, Y.: EnviSuM, Clean Shipping: Exploring the impact of emission
855   regulation, Final report, 2019. (available at: https://blogit.utu.fi/envisum/, 2020).

Rexeis, M., Hausberger, S., Kühlwein, J., and Luz, R.: Update of Emission Factors for EURO 5 and EURO 6 vehicles for the HBEFA Version 3.3, Report No. I-31/2013/ Rex EM-I 2011/20/679 from 06.12.2013, Graz University of Technology, Switzerland. (http://www.hbefa.net/e/documents/HBEFA33_Documentation_20170425.pdf, accessed 10/6 2018).

Segersson, D., Eneroth, K., Gidhagen, L., Johansson, C., Omstedt, G., Nylén, A.E., and Fosberg, B.: Health impact of PM_{10}, $PM_{2.5}$ and black carbon exposure due to different source sectors in Stockholm, Gothenburg and Umea, Sweden, Int. J. Environ. Res. Public Health, 14, 742, dio:10.3390/ijerph14070742, 2017.

SMED: Description of Methods and Quality of Spatially Distributed Emissions to Air, 2015. Contract no 309 1235.

Sofiev, M., Siljamo, P., Valkama, I., Ilvonen, M., and Kukkonen, J.: A dispersion mod-elling system SILAM and its evaluation against ETEX data, Atmos. Environt 40(4), 674–685, 2006.

Sofiev, Mikhail; Winebrake, James J.; Johansson, Lasse; Carr, Edward W.; Prank, Marje; Soares, Joana et al. (2018): Cleaner fuels for ships provide public health benefits with climate tradeoffs. In Nature communications 9 (1), p. 406. DOI: 10.1038/s41467-017-02774-9.

Thunis, P., Pederzoli, A., and Pernigotti, D.: Performance criteria to evaluate air quality modeling applications. Atmos. Environ., 79, 476–482, 2012.

Winnes, H., Styhre, L., and Fridell, E.: Reducing GHG emissions from ships in port areas, Res. Trans. Bus. Manage., 73–82, 2015.

WHO 2013a. Health risks of air pollution in Europe – HRAPIE project: Recommendations for concentration–response functions for cost–benefit analysis of particulate matter, ozone and nitrogen dioxide. http://www.euro.who.int/__data/assets/pdf_file/0006/238956/Health_risks_air_pollution_HRAPIE_project.pdf (assessed 2019-10-21)

WHO 2013b. Review of evidence on health aspects of air pollution – REVIHAAP project: final technical report. http://www.euro.who.int/en/health-topics/environment-and-health/air-quality/publications/2013/review-of-evidence-on-health-aspects-of-air-pollution-revihaap-project-final-technical-report (assessed 2019-10-16)
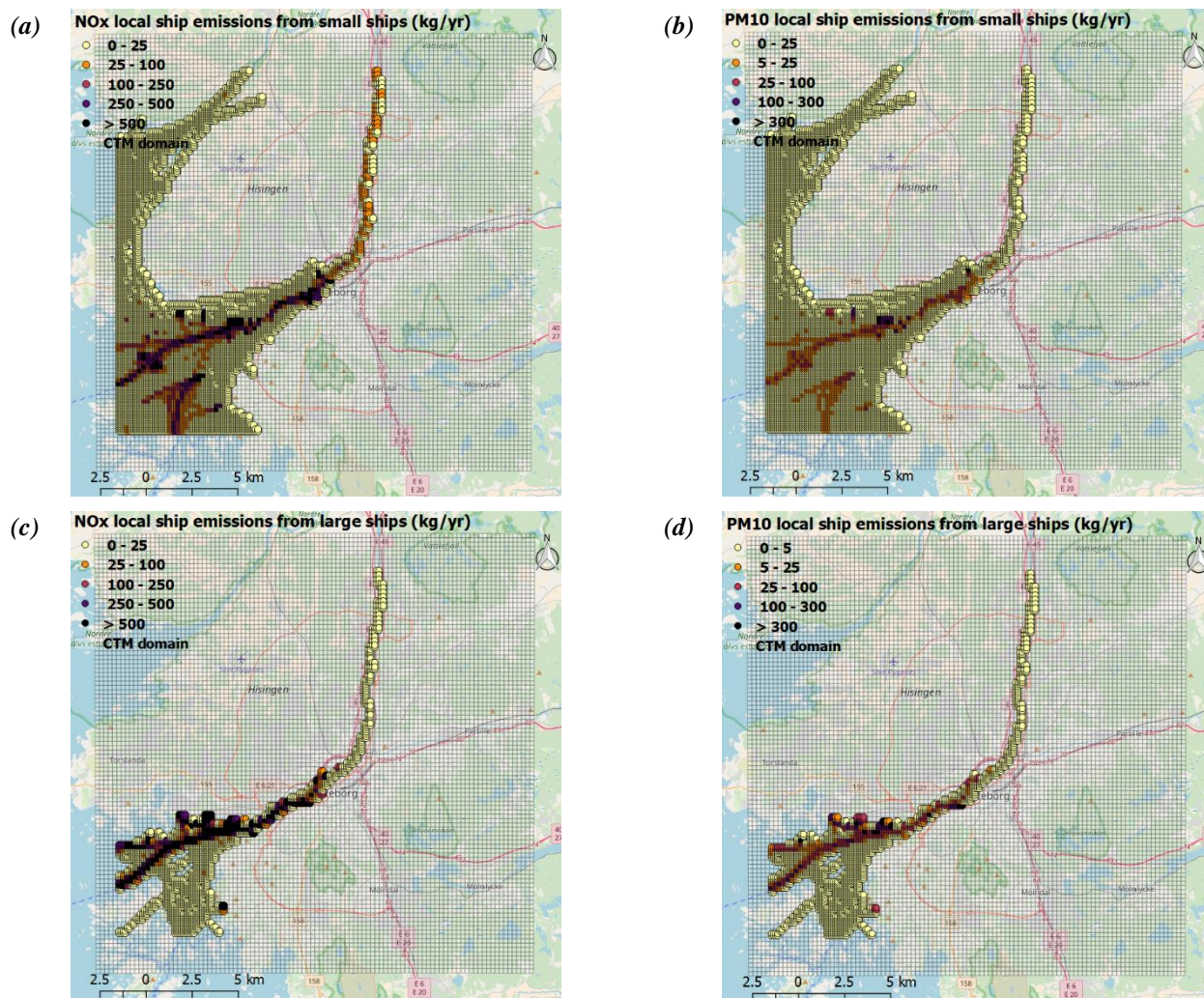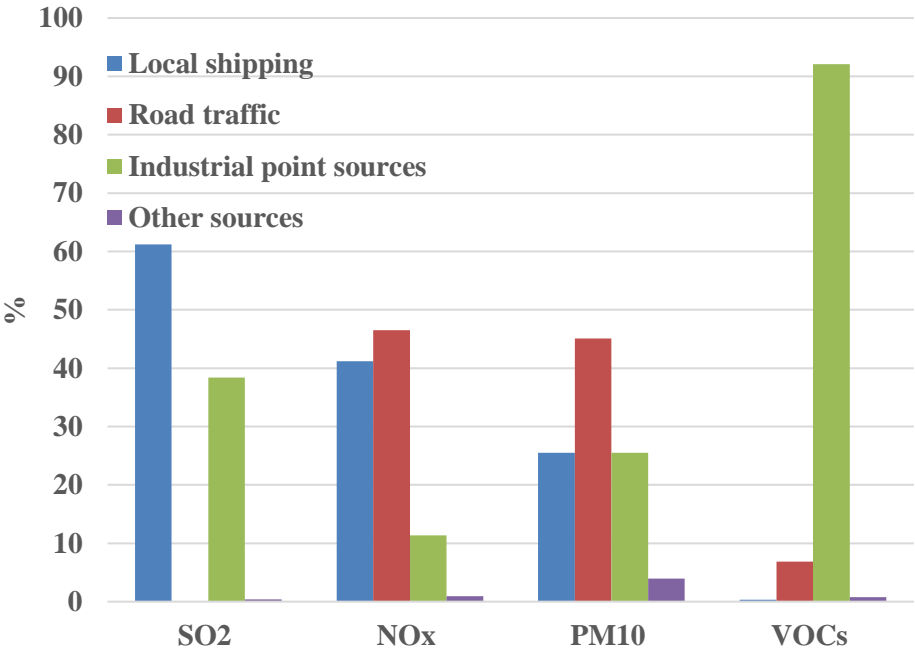
a)

(b)

Figure 1: (a) Five nested meteorological model domains with their sizes and spatial resolutions. The fifth domain with air pollution grid (250×250 m^2) is pointed out in the figure, showing location of the three air quality monitoring sites Femman, Haga and Mölndal, as well as Eriksberg, a residential are close to the harbour; (b) The boundary conditions of air pollution in TAPM, example of summer mean (JJA) year 2012 NO_2 concentrations [ppbV] in the regional-scale CMAQ simulation (4×4 km^2). Base map credits: © OpenStreetMap contributors (openstreetmap.org). Distributed under a Creative Commons BY-SA License.

885   **Figure 2: Annual local shipping emissions of (a) NO$_x$ and (b) PM$_{10}$ (equal to PM$_{2.5}$) from small vessels with stack height below 36 m (assumed 15 m) and (c) NO$_x$ and (d) PM$_{10}$ from large vessels with high stacks height above 36 m (assumed 36 m) in the Gothenburg area. Base map credits: © OpenStreetMap contributors (openstreetmap.org). Distributed under a Creative Commons BY-SA License.**

890

Figure 3: Proportions of different source categories in the local emission inventory for the city-scale model domain in year 2012. The total emissions are 502 tons year^{-1} for SO$_2$, 5072 tons year^{-1} for NO$_x$, 357 tons year^{-1} for PM$_{10}$ and 7457 tons year^{-1} for VOCs.

895

(a)　　　Wind rose plots of measurements at Femman station

(b)

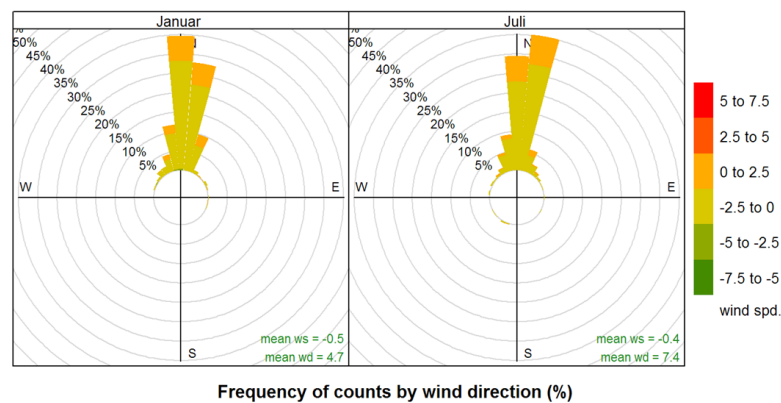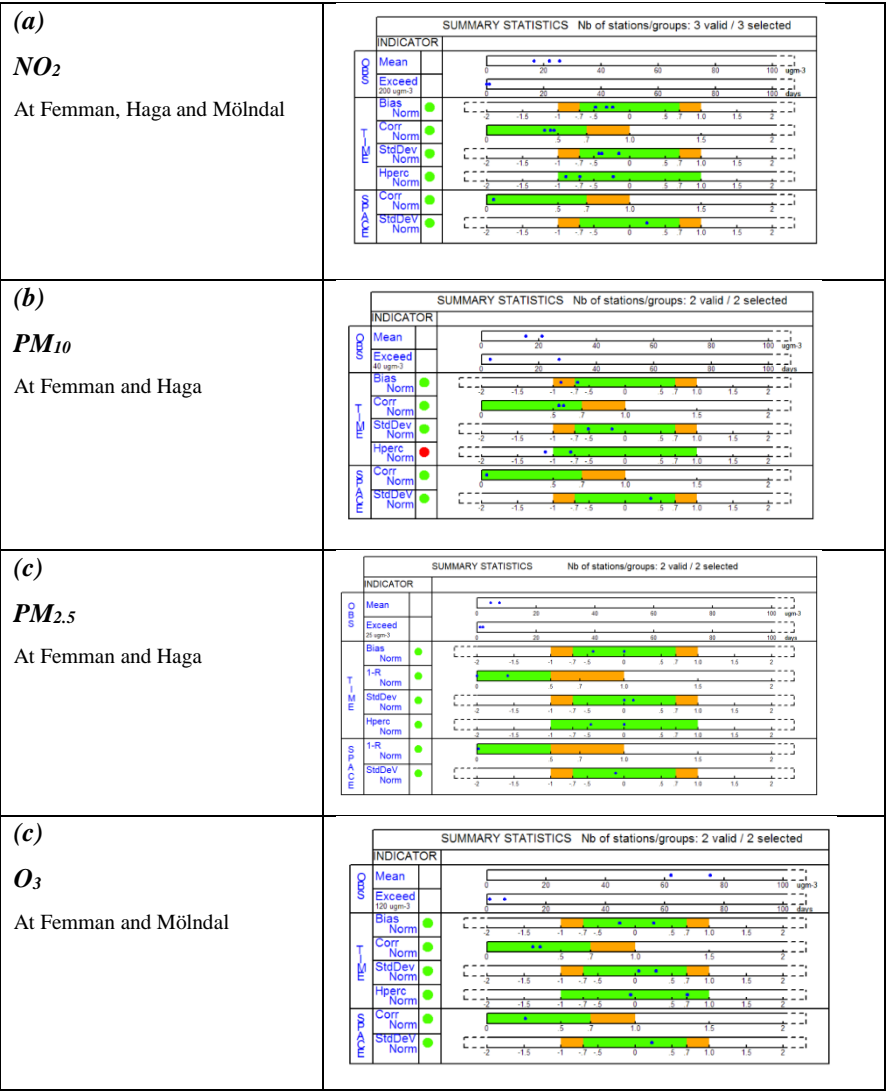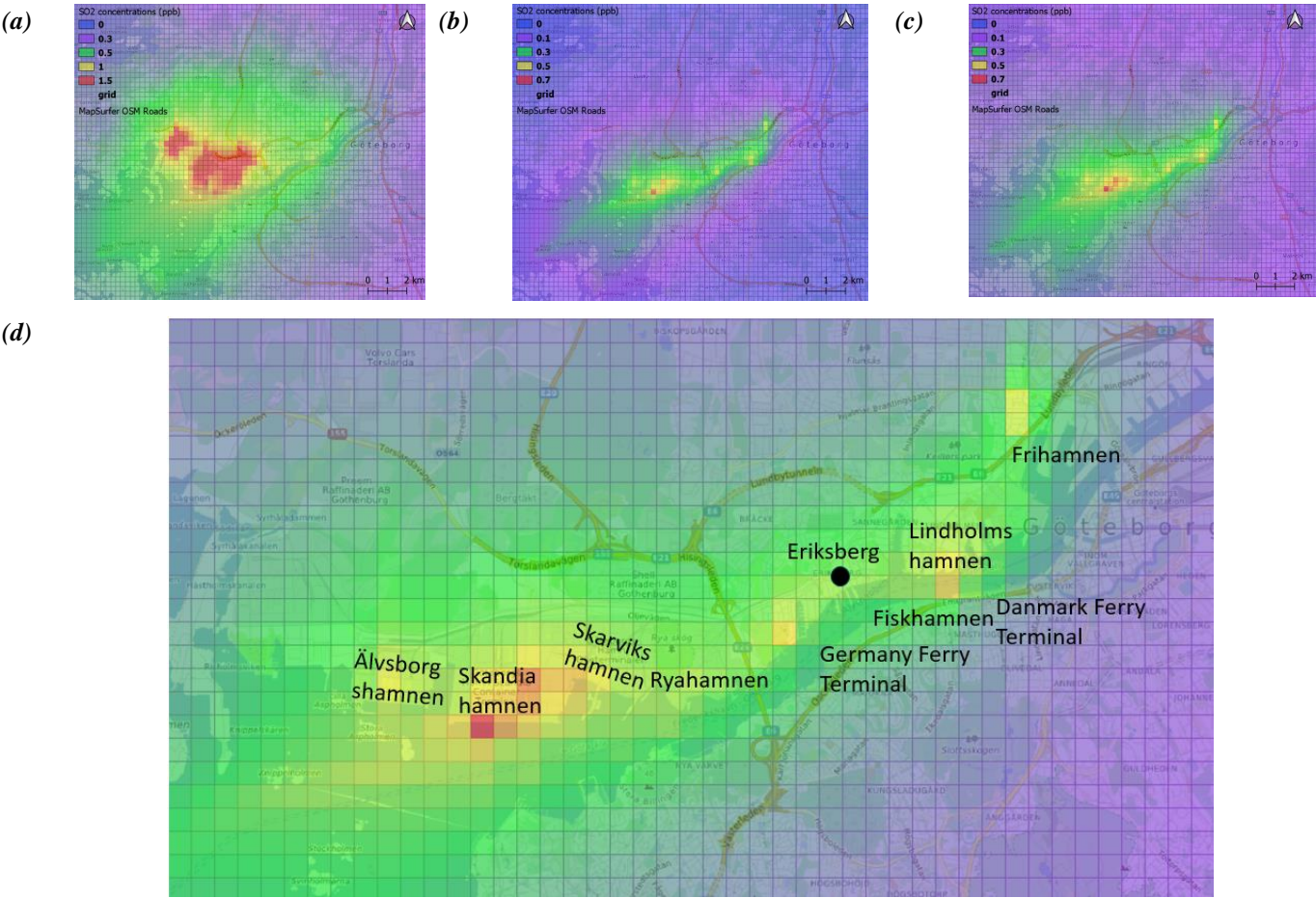Difference wind rose plots at Femman station

Figure 4: Comparison between measured and modelled winds at Femman station: (a) the observed wind rose in January and July; (b) BIAS of the wind speed based on the difference simulated wind speed – measured wind speed. E.g. a positive BIAS from 0 to 2.5 m s^{-1} in wind direction N has a frequency of almost 30 %.

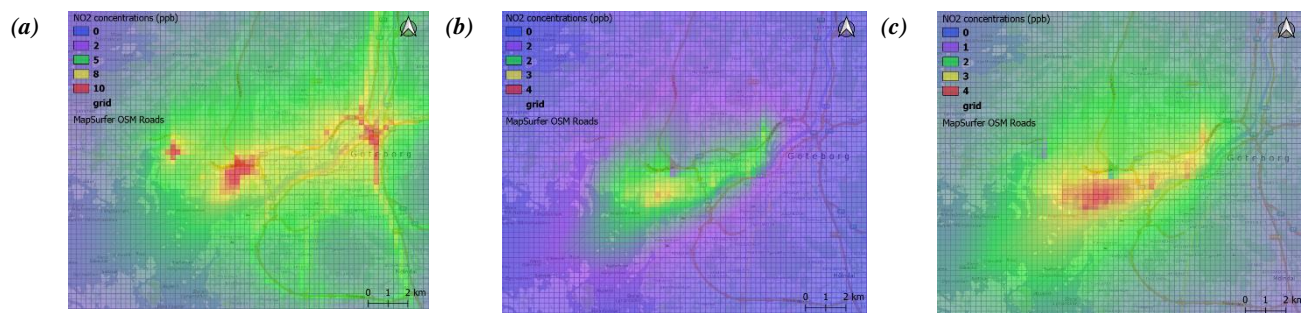|	
(a) *NO₂* At Femman, Haga and Mölndal	
(b) *PM₁₀* At Femman and Haga	
(c) *PM₂.₅* At Femman and Haga	
(c) *O₃* At Femman and Mölndal	

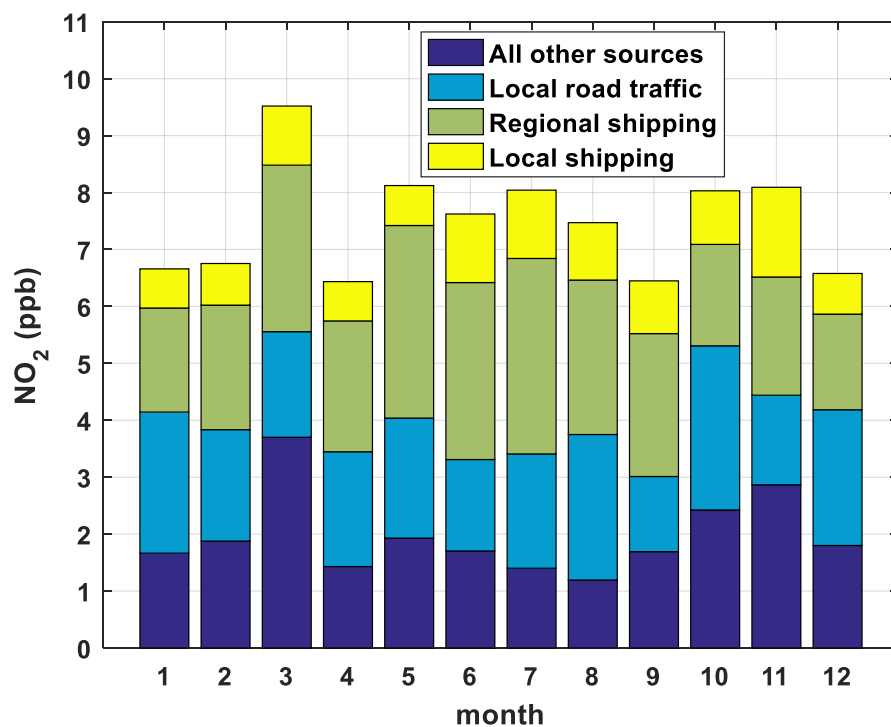**Figure 5: Summary statistics of model performance for the annual mean values of (a) NO₂ (hourly values), (b) PM₁₀ (daily values), (c) PM₂.₅ (daily values), and (d) O₃ (daily maximum of the 8-hour means), including days of exceedances. Stations (blue dots) within green bar: performance criteria satisfied, stations within orange bar: performance criteria satisfied, error dominated by the corresponding indicator. Green light: > 90 % of the stations fulfil the performance criteria. Red light: < 90 % of the stations fulfil the performance criteria. The indicator Hperc indicates the model capability to reproduce extreme events, represented by selected high percentile for modelled and observed values.**

Figure 6: Simulated atmospheric concentrations of SO₂ (in ppb) for year 2012: (a) Annual mean concentrations in Base case simulation; (b) Annual mean contribution of the local shipping; (c) Annual mean contribution of the local and the regional shipping; and (d) Same as (c) with main ports along the Göta älv as well as Eriksberg. Base map credits: © OpenStreetMap contributors (openstreetmap.org). Distributed under a Creative Commons BY-SA License.
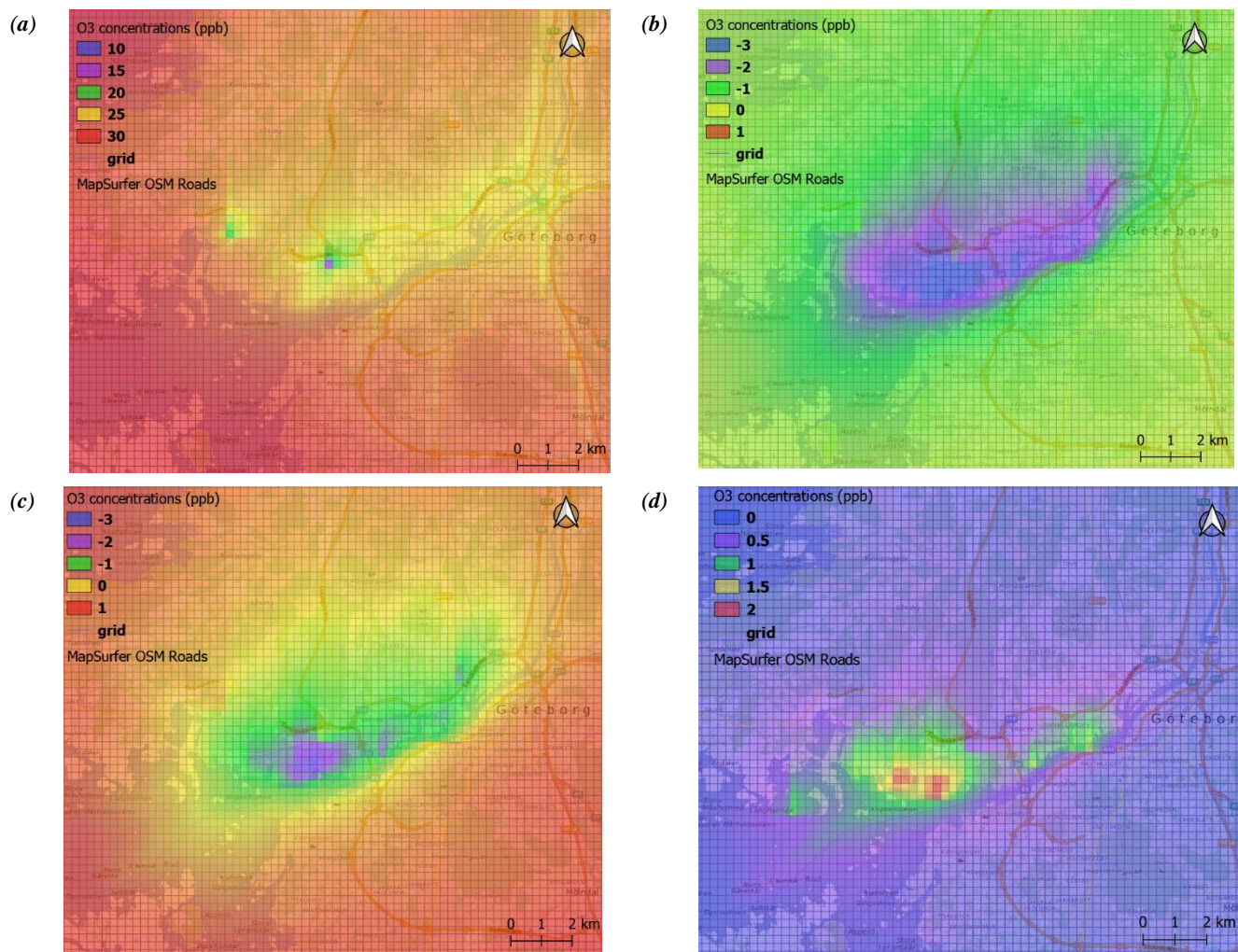
Figure 7: Simulated atmospheric concentrations of NO₂ (in ppb) for year 2012: (a) Annual mean concentrations in Base case simulation; (b) Annual mean contribution of the local shipping; (c) Annual mean contribution of the local and the regional shipping. Base map credits: © OpenStreetMap contributors (openstreetmap.org). Distributed under a Creative Commons BY-SA License.
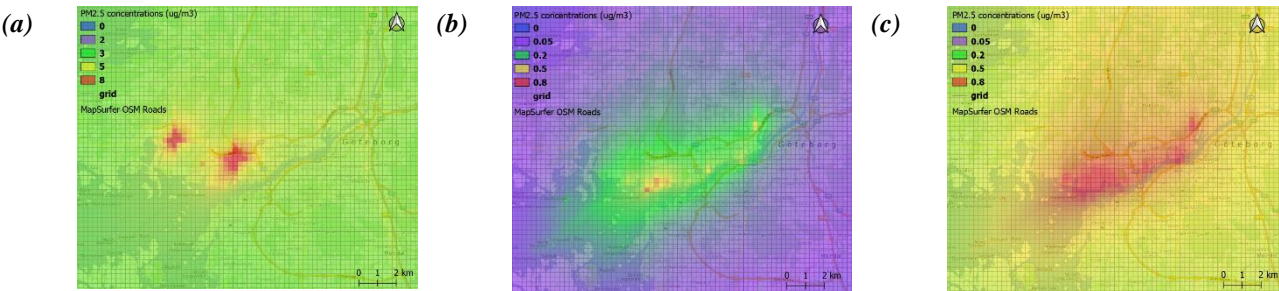
920

Figure 8: Modelled monthly mean contributions of the local shipping, regional shipping, local road traffic and other anthropogenic emissions (including contribution from the boundary conditions) to the NO₂ concentrations at Eriksberg in year 2012.
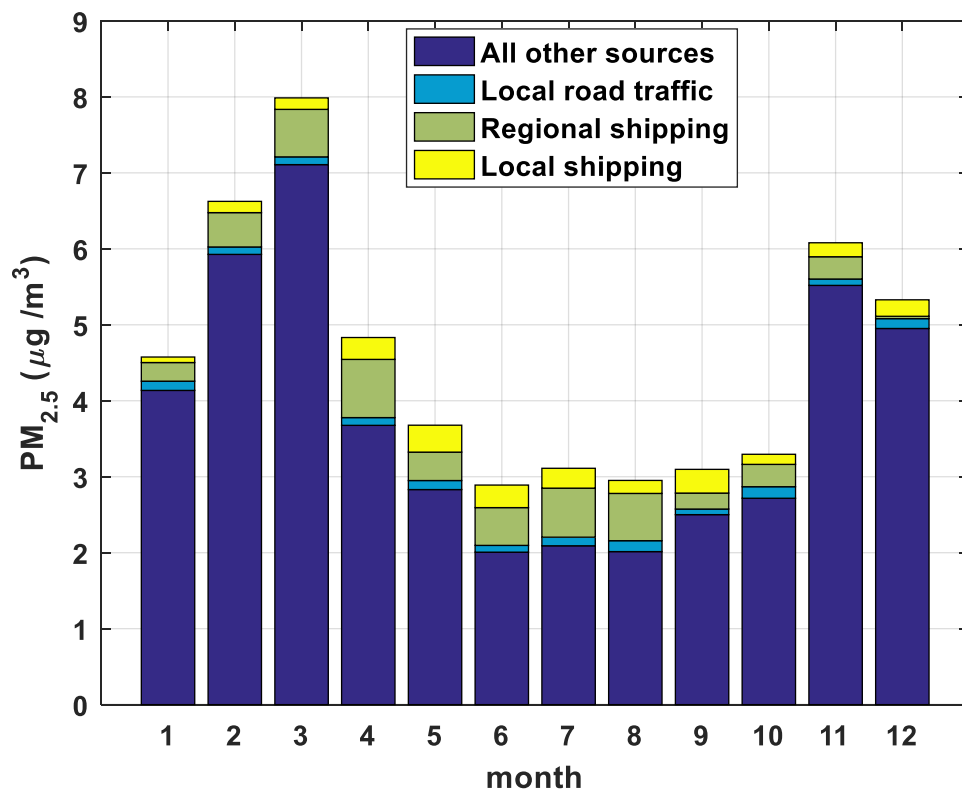
Figure 9: Modelled summer mean (JJA) ozone concentrations (ppb) in year 2012 and contributions of local and regional shipping:
(a) Modelled O₃ concentrations in the Base model simulation; (b) Modelled contribution of emissions from local shipping; (c) Modelled contribution of emissions from local and regional shipping; (d) Modelled contributions of NMVOC emissions from local shipping. Base map credits: © OpenStreetMap contributors (openstreetmap.org). Distributed under a Creative Commons BY-SA License.

930

Figure 10: Modelled annual mean PM$_{2.5}$ concentrations (µg m^{-3}) and contributions of shipping in year 2012: (a) Modelled annual mean concentrations in Base model simulation; (b) Modelled annual mean contribution of local shipping; (c) Modelled annual mean contributions of local and regional shipping. Base map credits: © OpenStreetMap contributors (openstreetmap.org). Distributed under a Creative Commons BY-SA License.
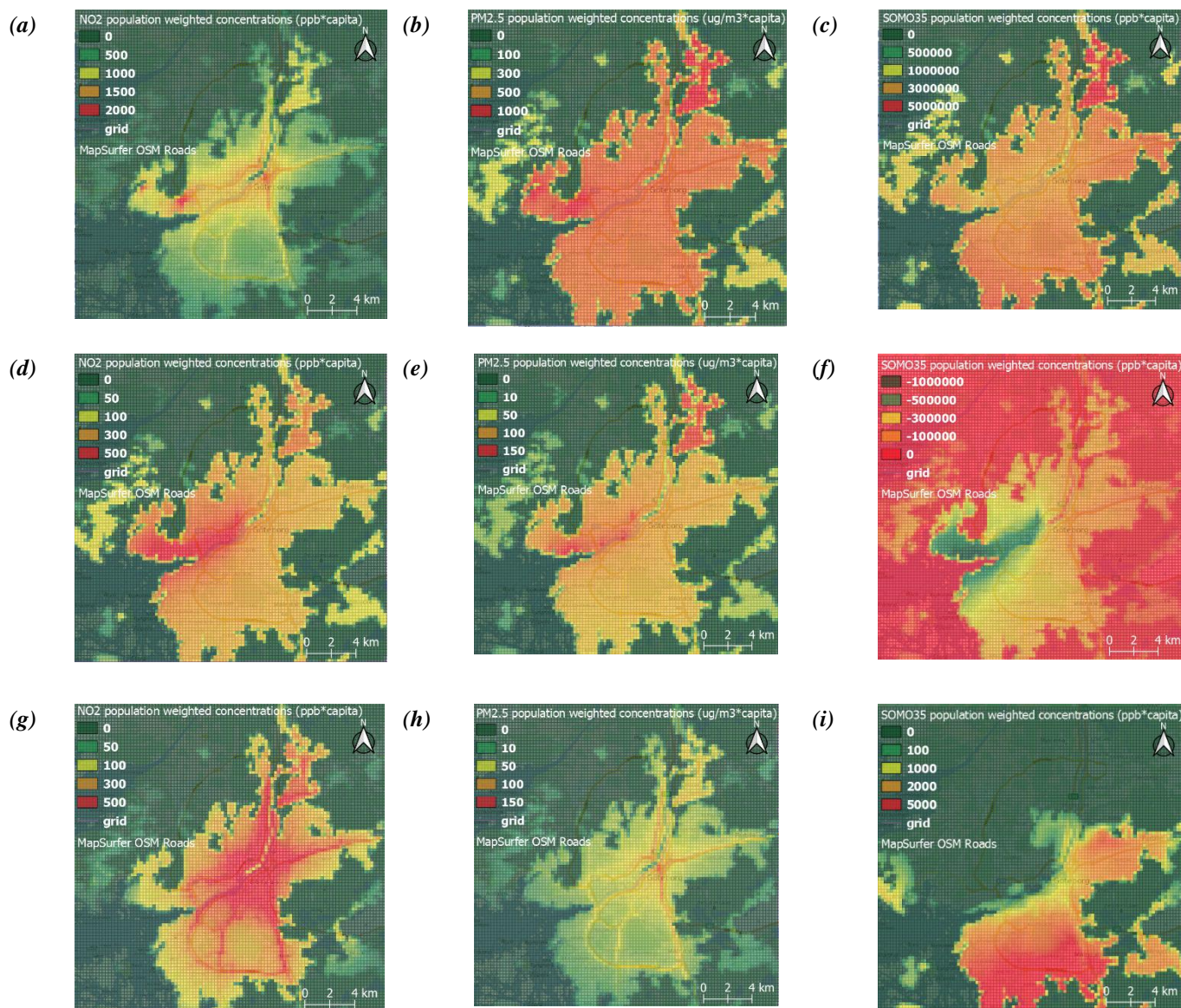
935

Figure 11: Modelled monthly mean contributions from local shipping, regional shipping and other sources (including contribution from the boundary condition) to PM$_{2.5}$ concentrations at Eriksberg for year 2012.

Figure 12: The population weighted annual mean concentrations for NO₂ (ppb × capita), PM₂.₅ (µg m⁻³ × capita) and SOMO35 (ppb × h × capita): (a) NO₂ in the Base simulation; (b) PM₂.₅ in the Base simulation; (c) SOMO35 in the Base simulation; (d) NO₂ from local and regional shipping; (e) PM₂.₅ from local and regional shipping; (f) SOMO35 from local and regional shipping; (g) NO₂ from road traffic; (h) PM₂.₅ from road traffic and (i) SOMO35 from road traffic. Base map credits: © OpenStreetMap contributors (openstreetmap.org). Distributed under a Creative Commons BY-SA License.

Table 1: City-scale model setup.

	Domain	Spatial resolutions	Model / Database
Meteorology	30 km × 30 km	500 m	ECMWF ERA5 0.3˚ × 0.3˚, 21 layers
Background concentrations	160 km × 96 km	4 km × 4 km	CMAQ
Local shipping emissions	30 km × 30 km	250 m × 250 m	STEAM2
Local traffic emissions	30 km × 30 km	meters (line sources)	Miljöförvaltningen and HBEFA v. 3.2
Local industrial, machines, wood burning and aviation *etc*.	30 km × 30 km	1 km × 1 km	SMED

Table 2: Population weighted annual mean concentrations of NO_2, $PM_{2.5}$ and SOMO35 associated to all sources, road traffic and local, regional shipping in city of Gothenburg for year 2012.

Sources	NO_2 (ppb)	$PM_{2.5}$ ($\mu g\ m^{-3}$)	SOMO35 (ppb × h)
PWC in Base simulation	4.70	4.12	19 698
Road traffic	1.75	0.22	12
Local and regional shipping	1.65	0.51	-1 115
Local shipping	0.68	0.09	-1 186
Regional shipping	0.97	0.42	71

Table 3: Health impacts calculated for O_3, NO_2 and $PM_{2.5}$ contributions of the local and regional shipping and the local road traffic to air pollution in the city of Gothenburg as well as of the total exposure to these pollutants in the city. The health impacts calculated with the ARP model and with the RAINS methodology are presented.

Pollutant	Impact	Unit	Local shipping	NSBS regional shipping	All shipping	Local road traffic	Total exposure
O_3	Acute Mortality (All ages)	Premature deaths	-0.5	0.03	-0.4	0.005	7.6
NO_2	Acute Mortality (All ages)	Premature deaths	1.06	1.52	2.59	2.73	7.35
$PM_{2.5}$	Chronic Mortality (All ages)	Life years lost	31	143	174	74	1393
	Chronic mortality (All ages, ARP)	YOLLs pers. $^{-1}$	0.003	0.013	0.015	0.007	0.12
	Chronic Mortality (Age 30+, RAINS)	YOLLs pers. $^{-1}$	0.003	0.014	0.018	0.008	0.14
	Chronic mortality relative to that from the total exposure	-	2 %	10 %	12 %	5 %	